

UNIVERSITÀ DEGLI STUDI
DI NAPOLI FEDERICO II

Farid Ahmadi

Numerical and Analytical Investigation of FRP-to-Masonry Bond Behaviour Considering Mortar Joint Discontinuities



FRP++
Advanced structural analysis and design using composite materials

Master Dissertation
European Master Advanced Structural Analysis and Design using Composite Materials

Work developed under the supervision of
Professor Gian Piero Lignola



Funded by
the European Union

July 2026

DECLARATION

Name: Farid Ahmadi

Email: farid.ahmadi.jp@gmail.com **Phone number:** +393479214774

Citizen Card Number: XXXXXXXXXXXXXXXXXXX

Title of the Thesis: Numerical and Analytical Investigation of FRP-to-Masonry Bond Behaviour Considering Mortar Joint Discontinuities

Supervisors:

Professor Gian Piero Lignola

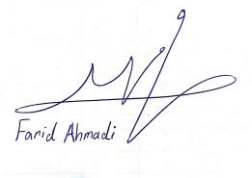
Year of Conclusion: 2026

Master Course in Advanced Structural Analysis and Design using Composite Materials

THE ENTIRE REPRODUCTION OF THIS THESIS IS AUTHORIZED ONLY FOR RESEARCH PURPOSES, UPON WRITTEN DECLARATION BY THE INTERESTED PERSON, WHICH IS COMMITTED TO.

University of Naples Federico II, 22/07/2026

Signature:



ACKNOWLEDGEMENTS

First and foremost, I would like to express my sincere gratitude to my supervisor, Professor Gian Piero Lignola, for his invaluable guidance, continuous support, and insightful advice throughout every stage of this research. His expertise, constructive feedback, and encouragement have been instrumental in shaping this dissertation and deepening my understanding of FRP-strengthened masonry systems. I am truly grateful for the time, patience, and dedication he devoted to this work.

I would also like to express my sincere appreciation to all the professors and academic staff of the FRP++ Joint Master's Programme for providing an exceptional learning environment and sharing their knowledge and experience throughout this unique academic journey. Their commitment to excellence has significantly contributed to both my academic and professional development.

I am deeply grateful to the FRP++ Consortium for awarding me a scholarship that covered the tuition fees of my master's studies. This generous support made it possible for me to pursue this unique international academic journey, study at leading European universities, and broaden both my academic and professional horizons.

My heartfelt gratitude goes to my parents for their unconditional love, endless encouragement, and unwavering belief in me. Their sacrifices, patience, and continuous support have been the foundation of my academic journey and the driving force behind every achievement. I owe this accomplishment to their constant motivation and confidence in my abilities.

Finally, I would like to thank Almighty God for granting me the strength, perseverance, and opportunities to complete this important milestone. I am truly grateful for His guidance throughout this journey and for every challenge that has contributed to my personal and professional growth.

Indagine Numerica e Analitica del Comportamento di Aderenza tra FRP e Muratura in Presenza di Discontinuità nei Giunti di Malta

RIASSUNTO

I compositi in Polimero Rinforzato con Fibre (FRP) sono ampiamente utilizzati per il rinforzo delle strutture in muratura grazie alle elevate prestazioni meccaniche, alla resistenza alla corrosione e alla facilità di applicazione. Tuttavia, l'efficacia dei sistemi FRP incollati esternamente è spesso limitata dal distacco prematuro all'interfaccia FRP–muratura, mentre l'influenza delle discontinuità dei giunti di malta sul meccanismo di trasferimento degli sforzi rimane ancora poco compresa. La maggior parte degli studi numerici considera infatti la muratura come un materiale omogeneo, trascurando gli effetti locali dei giunti di malta.

La presente tesi propone un'indagine analitica e numerica del comportamento di aderenza tra lamine FRP e substrati in muratura, con particolare attenzione all'influenza dei giunti di malta. È stato sviluppato un modello non lineare agli elementi finiti in ABAQUS utilizzando il modello Concrete Damage Plasticity per la muratura e una legge coesiva di tipo traction–separation per l'interfaccia. Dopo la validazione rispetto a risultati presenti in letteratura, il modello è stato impiegato per analizzare l'influenza della rigidezza assiale dell'FRP, del tipo di substrato, della lunghezza di aderenza, dello spessore dei giunti di malta e delle proprietà meccaniche della muratura. I risultati numerici sono stati inoltre confrontati con le previsioni analitiche basate sulle linee guida CNR-DT 200.

I risultati mostrano che l'aumento della rigidezza assiale dell'FRP determina un incremento della lunghezza efficace di aderenza, mentre i giunti di malta interrompono localmente il trasferimento degli sforzi, causando una redistribuzione delle tensioni e un'estensione della lunghezza efficace. Inoltre, la riduzione della capacità di aderenza dipende principalmente dal rapporto tra la lunghezza di aderenza disponibile e quella efficace, piuttosto che dal solo spessore dei giunti. I substrati in laterizio risultano più sensibili alla presenza dei giunti di malta rispetto a quelli in tufo, a causa della loro minore lunghezza efficace di aderenza. Il

modello proposto contribuisce a una migliore comprensione del comportamento di aderenza FRP–muratura e supporta la progettazione di sistemi di rinforzo per murature eterogenee.

PAROLE CHIAVE: Aderenza FRP–Muratura; Rinforzo di Murature; Discontinuità dei Giunti di Malta; Lunghezza Efficace di Aderenza; Distacco Interfacciale.

Numerical and Analytical Investigation of FRP-to-Masonry Bond Behaviour Considering Mortar Joint Discontinuities

ABSTRACT

Fiber Reinforced Polymer (FRP) composites are widely used for strengthening masonry structures due to their high mechanical performance, corrosion resistance, and ease of application. However, the effectiveness of externally bonded FRP systems is often limited by premature debonding at the FRP–masonry interface, while the influence of mortar joint discontinuities on the stress-transfer mechanism remains insufficiently understood. Most existing numerical studies idealize masonry as a homogeneous material, neglecting the local effects of mortar joints.

This dissertation presents a combined analytical and numerical investigation of the bond behaviour of externally bonded FRP strips to masonry substrates, with particular emphasis on mortar joint discontinuities. A nonlinear finite element model was developed in ABAQUS using the Concrete Damage Plasticity model for masonry and a cohesive traction–separation law for the interface. After validation against published results, the model was employed to investigate the influence of FRP axial stiffness, substrate type, bond length, mortar thickness and masonry mechanical properties, and the results were compared with analytical predictions based on the CNR-DT 200 design provisions.

The results demonstrate that increasing FRP axial stiffness increases the effective bond length, while mortar joints locally interrupt the stress-transfer mechanism, causing stress redistribution and extension of the effective bond length. Furthermore, the reduction in bond capacity is governed primarily by the relationship between the available and effective bond lengths rather than by mortar thickness alone. Brick substrates were found to be more sensitive to mortar joints than stone substrates due to their shorter effective bond lengths. The proposed framework provides improved insight into FRP-to-masonry bond behaviour and supports the design of strengthening systems for heterogeneous masonry.

KEYWORDS: FRP-to-Masonry Bond; Masonry Strengthening; Mortar Joint Discontinuities; Finite Element Analysis; Effective Bond Length; Debonding.

TABLE OF CONTENTS

Acknowledgements III

Indagine Numerica e Analitica del Comportamento di Aderenza tra FRP e Muratura in Presenza di Discontinuità nei Giunti di Malta IV

Riassunto IV

Abstract VI

Table of Contents VII

List of Figures IX

List of Tables XII

List of Abbreviations and Symbols XIII

1. Introduction 1

1.1. Background on FRP Strengthening of Masonry Structures 1

1.2. Research Motivation and Gap 3

1.3. Aim and Objectives 5

1.3.1. Scope and Limitations 5

1.3.2. Significance of the Study 6

1.4. Structure of the Dissertation 7

2. Literature Review 9

2.1. Masonry structures and strengthening techniques 9

2.2. FRP Composites in Masonry Rehabilitation 10

2.3. Bond Behaviour of FRP-to-Masonry Systems 12

2.4. Failure Mechanisms and Debonding Phenomena 16

2.5. Experimental Single-Lap Shear Tests 19

2.6. Interface Modelling and Bond-Slip Behaviour 22

2.7. Numerical Modelling of FRP-to-Masonry Bond Behaviour 24

2.8. Research Gaps and Objectives of the Present Study 26

3. Methodology 29

3.1. Overview 29

3.2. Analytical Formulation of FRP-to-Masonry Bond Behaviour 30

3.2.1. Equilibrium and Compatibility Relationships 31
3.2.2. Bond-Slip Constitutive Relationships 31
3.2.3. Effective Bond Length and Debonding Resistance 32
3.2.4. Representation of Masonry Discontinuities 33
3.3. Finite Element Modelling of FRP-to-Masonry 33
3.3.1. Geometry and Model Configuration 34
3.3.2. Constitutive Modelling of Masonry and FRP Materials 36
3.3.3. Interface Modelling and Cohesive Behaviour 39
3.3.4. Boundary Conditions and Loading Procedure 42
3.3.5. Mesh Discretization and Element Types 43
3.4. Model Validation 44
..... 45
4. Results and Discussions 47
4.1. FRP Strip Bonded to Homogeneous substrate 47
4.1.1. Influence of FRP Axial Stiffness and Substrate Properties on Bond Behaviour . 48
4.1.2. Interfacial Stress Transfer Mechanism and Effective Bond Length 50
4.2. Influence of Mortar Joints on the FRP–Masonry Bond Mechanism 54
4.2.1. Overall Influence of Mortar Joints on Bond Capacity 55
4.2.2. Effect of Mortar Joints on the Global Bond Response 56
4.2.3. Effect of Mortar Joints on the Stress-Transfer Mechanism 57
4.2.4. Effect of Mortar Joints Under Different Bond Length Conditions 60
4.2.5. Influence of FRP Axial Stiffness and Mortar Joints on Bond Failure Brittleness 64
5. Conclusions and Further Developments 67
5.1. Conclusions 67
5.2. Original Contributions of the Present Study 69
5.3. Further Developments 70
References 73

LIST OF FIGURES

Figure 2.1: Different FRP strip strengthening configurations used in masonry rehabilitation [13]. 10
Figure 2.2: Strengthening of masonry wall using externally bonded FRP laminates [18]. 11
Figure 2.3: Numerical simulation of debonding propagation and stress concentration in FRP-strengthened masonry systems [11]. 13
Figure 2.4: Typical failure modes in FRP-strengthened masonry systems: (a) flexural-shear debonding failure and (b) shear failure [14]. 14
Figure 2.5: FE simulation of FRP delamination from masonry for different FRP width-to-masonry width ratios: (a) narrow FRP strip and (b) wide FRP strip [20]. 15
Figure 2.6: Debonding test results for a representative masonry specimen showing the failure mode and the distributions of longitudinal strain and displacement along the bonded interface at different load levels [11]. 17
Figure 2.7: Crack distribution and debonding propagation in FRP-strengthened masonry specimens for different FRP width-to-masonry width ratios 18
Figure 2.8: Experimental setup of a single-lap shear test for investigating the bond behaviour between composite reinforcement and masonry substrate [22]. 20
Figure 2.9: Experimental setup of a bond test performed on a strengthened masonry specimen during single-lap shear loading [24]. 21
Figure 2.10: Schematic representation of the interface constitutive law used for modelling the nonlinear bond-slip behaviour of FRP interfaces [22]. 23
Figure 2.11: Comparison between experimental and predicted bond strength values using different machine learning and regression models for FRP-to-masonry bond behaviour prediction [26]. 24
Figure 2.12: Micro-mechanical finite element model and boundary conditions for FRP-strengthened curved masonry specimens subjected to single-lap shear tests [27]. 25

Figure 3.1: Schematic illustration of the bonded FRP-to-masonry system used for the analytical bond formulation. 30
Figure 3.2: Schematic representation of bond-slip constitutive relationship and interface law 31
Figure 3.3 Inelastic mechanical properties adopted for the constituent materials assuming uniaxial compression [27]: (a) uniaxial compressive behaviour; (b) uniaxial tensile behaviour. [27]. 38
Figure 3.4: Boundary conditions and displacement-controlled loading configuration adopted in the finite element model. 42
Figure 3.5: (a) Meshed finite element model; (b) Zoomed view of compatible mesh discretization at the bonded interface. 44
Figure 3.6: Reference numerical load–displacement responses reported by Bertolesi et al. [27] 45
Figure 3.7: Load–displacement responses obtained from the present finite element validation model. 45

Figure 4.1: Schematic of FRP strip bonded to homogeneous substrate. 47
Figure 4.2: Effect of substrate and FRP system on the load–displacement response. 48
Figure 4.3: Comparison between the FE numerical results and the CNR analytical predictions for the peak bond load as a function of FRP axial stiffness. 49
Figure 4.4: Stress redistribution associated with the interfacial shear stress distribution. 51
Figure 4.5: Evolution of the interfacial shear stress distribution during debonding. 52
Figure 4.6: Interfacial shear stress distribution for different FRP–substrate combinations. .. 52
Figure 4.7: Comparison between the effective bond lengths obtained from the finite element (FE) simulations and the corresponding predictions from the CNR analytical formulation for different FRP axial stiffness values. 53
Figure 4.8: Peak load capacity as a function of FRP axial stiffness for different substrates and mortar thicknesses. 55
Figure 4.9: Effect of substrate and FRP system on the load–displacement response for the thickest masonry mortar layer. 56

Figure 4.10: Interfacial shear stress distribution for different FRP–substrate combinations at the maximum masonry mortar thickness. 58
Figure 4.11: Stress redistribution associated with the interfacial shear stress distribution at with mortar effect. 59
Figure 4.12: Evolution of the interfacial shear stress distribution during debonding at the maximum masonry mortar thickness. 60
Figure 4.13: Effect of masonry mortar thickness on the load–displacement response and interfacial shear stress distribution for (a) BL > EBL, (b) BL ≈ EBL, and (c) BL < EBL. 61
Figure 4.14: Effect of bond length and masonry mortar thickness on peak load capacity. 62
Figure 4.15: Effect of masonry mortar thickness on peak load reduction for different bond lengths. 63
Figure 4.16: Effect of masonry mortar thickness on the effective bond length..... 64
Figure 4.17: Influence of masonry mortar thickness on the bond failure characteristics: (a) reduction in interface slip capacity; (b) bond brittleness index. 65
Figure 4.18: Effect of FRP axial stiffness and masonry mortar thickness on slip Capacity (at Failure)..... 66

LIST OF TABLES

Table 3.1: Geometrical properties of the finite element model. 35

Table 3.2: Elastic material properties adopted for the finite element model. 36

Table 3.3: Cohesive interface properties adopted in the finite element model. 40

Table 4.1: Comparison between the FE numerical results and the CNR analytical predictions of peak bond load 49

Table 4.2: Comparison between the FE numerical results and the CNR analytical predictions for the effective bond length of different FRP–substrate combinations. 54

LIST OF ABBREVIATIONS AND SYMBOLS

Abbreviations

ABAQUS	Finite Element Analysis Software
AFRP	Aramid Fibre Reinforced Polymer
BL	Bond Length
BFRP	Basalt Fibre Reinforced Polymer
CDP	Concrete Damage Plasticity
CFRP	Carbon Fibre Reinforced Polymer
CNR	Advisory Committee on Technical Recommendations for Construction
CRM	Composite Reinforced Mortar
CZM	Cohesive Zone Model
EB	Externally Bonded
EBL	Effective Bond Length
FE	Finite Element
FEM	Finite Element Method
FRP	Fibre Reinforced Polymer
GFRP	Glass Fibre Reinforced Polymer
HMFRP	High Modulus Carbon Fibre Reinforced Polymer
MAXS	Maximum Nominal Stress Damage Initiation Criterion
NSM	Near-Surface Mounted
RP	Reference Point
URM	Unreinforced Masonry

Symbols

b_f	Width of FRP strip
E_f	Elastic modulus of FRP reinforcement
F_{max}	Maximum transferable force
G_f	Fracture energy
K_{nn}	Normal interface stiffness coefficient
K_{ss}	Shear interface stiffness coefficient
K_{tt}	Secondary shear interface stiffness coefficient
L_b	Bonded length
t_f	Thickness of FRP strip
$T_{(z)}$	Axial force in FRP reinforcement
$u_{f(z)}$	Axial displacement of FRP reinforcement
$u_{m(z)}$	Axial displacement of masonry substrate
z	Coordinate along the bonded interface
ε_f	Axial strain of FRP reinforcement
Γ_f	Interface fracture energy
ν	Poisson's ratio
τ	Interfacial shear stress
$\tau_{(z)}$	Shear stress distribution along the bonded interface
$\tau_{(s)}$	Bond-slip constitutive relationship
σ	Normal stress
E_m	Elastic modulus of mortar
L_e	Effective bond length
t_m	Mortar thickness
F	Applied load
X	Longitudinal coordinate
y	Vertical coordinate

1. INTRODUCTION

1.1. Background on FRP Strengthening of Masonry Structures

Masonry structures represent one of the oldest and most widely used construction systems in civil engineering. Their extensive application is mainly attributed to their durability, fire resistance, thermal insulation properties, architectural versatility, and economic efficiency [1]. Despite these advantages, masonry materials inherently exhibit low tensile strength and limited ductility, making them highly vulnerable to cracking and brittle failure under seismic and lateral loading conditions [2]. Masonry is also considered a heterogeneous material due to the combination of masonry units, mortar joints, grout, and reinforcement accessories, each possessing distinct mechanical properties. The discontinuous arrangement of mortar joints introduces local variations in stiffness and strength, which significantly influence stress transfer mechanisms and crack propagation behaviour within masonry systems [1].

A considerable portion of existing masonry structures, particularly unreinforced masonry (URM) buildings, were constructed without consideration of modern seismic design requirements. Consequently, many of these structures require strengthening and rehabilitation interventions to improve their structural safety, load-carrying capacity, and durability. Conventional retrofitting methods such as reinforced concrete jacketing, steel bracing, external post-tensioning, and steel plate bonding have been widely adopted over the years. However, these techniques often suffer from disadvantages including increased structural mass, corrosion susceptibility, geometric intrusion, and installation difficulties [1]. As a result, Fiber Reinforced Polymer (FRP) composites have emerged as an efficient and attractive alternative for strengthening masonry structures.

FRP materials consist of high-strength fibres embedded within polymeric resin matrices. Depending on the fibre type, FRP systems are generally classified as Glass Fiber Reinforced Polymer (GFRP), Carbon Fiber Reinforced Polymer (CFRP), and Aramid Fiber Reinforced Polymer (AFRP) [1]. These materials offer several advantages including high tensile strength, corrosion resistance, lightweight characteristics, rapid installation procedures, and minimal alteration to the original geometry of the structure. Due to these favourable properties, FRP strengthening systems have gained significant attention in the rehabilitation of both

reinforced and unreinforced masonry structures subjected to static and cyclic loading conditions [3,4].

Different FRP strengthening techniques have been proposed for masonry applications, including externally bonded reinforcement systems, near-surface mounted (NSM) reinforcement, post-tensioning systems, center-core reinforcement methods, and cement-based matrix grid systems [1]. Among these methods, externally bonded FRP laminates remain one of the most commonly adopted strengthening approaches due to their simplicity and effectiveness in improving the flexural and shear resistance of masonry walls. Experimental investigations conducted by Triantafillou [3] demonstrated that CFRP laminates significantly improve the in-plane shear capacity of masonry walls under low axial loading conditions. Similarly, Chuang et al. [4] reported substantial improvements in strength, ductility, and energy dissipation capacity of FRP-strengthened masonry walls subjected to cyclic loading. Tumialan and Nanni [5] further showed that externally bonded FRP laminates can significantly increase both the strength and ductility of URM walls, although debonding failures may occur at the FRP-to-masonry interface.

Despite the considerable advantages of FRP strengthening systems, premature debonding at the FRP-to-masonry interface remains one of the most critical failure mechanisms limiting the efficiency of these retrofitting techniques [5,6]. Several studies have reported that interfacial debonding often governs the ultimate capacity of FRP-strengthened masonry elements before full utilization of the FRP tensile strength occurs [6]. The bond behaviour is strongly influenced by the mechanical properties of masonry constituents, adhesive characteristics, substrate heterogeneity, and local stress concentrations near mortar joints. Roko et al. [6] observed that the bond performance between FRP laminates and masonry substrates is closely related to the surface characteristics and porosity of masonry units, which directly affect the adhesion quality of the epoxy interface.

Although extensive research has been conducted on FRP strengthening of masonry structures, many existing analytical formulations and numerical approaches idealize masonry as a homogeneous substrate, neglecting the influence of mortar joint discontinuities on stress redistribution and bond transfer mechanisms. However, mortar joints introduce localized stiffness variations that may alter interfacial shear stress distributions, affect effective bond length evolution, and influence the initiation and propagation of debonding damage. Therefore, a deeper understanding of FRP-to-masonry

bond behaviour considering mortar joint discontinuities is necessary for the development of more accurate numerical models and reliable analytical design formulations. The present research focuses on investigating the local and global effects of mortar joints on interfacial stress transfer, damage evolution, and effective bond length behaviour through advanced numerical and analytical modelling approaches.

1.2. Research Motivation and Gap

The strengthening and rehabilitation of existing masonry structures has become an important topic in structural engineering due to the large number of historical and unreinforced masonry constructions that are vulnerable to seismic actions, environmental degradation, and increasing service loads [7], [8]. Among the available retrofitting techniques, externally bonded Fiber Reinforced Polymer (FRP) systems have attracted significant attention because of their high strength-to-weight ratio, corrosion resistance, low invasiveness, and ease of installation. Experimental investigations have shown that FRP composites can significantly improve the strength, stiffness, and ductility of masonry elements subjected to both in-plane and out-of-plane loading conditions [2], [8].

Despite these advantages, the effectiveness of FRP strengthening systems is strongly governed by the bond behaviour between the FRP reinforcement and the masonry substrate [10]. Premature debonding of the FRP from masonry is frequently observed as one of the dominant failure mechanisms in strengthened masonry members [7], [11]. This debonding process generally initiates within a thin layer of masonry beneath the adhesive interface and progressively propagates along the bonded region, leading to a significant reduction in the load transfer capacity of the strengthening system [9]. Consequently, understanding the interfacial behaviour between FRP and masonry is essential for the reliable design and assessment of strengthened masonry structures.

Many analytical and numerical studies available in the literature have investigated FRP-to-masonry bond behaviour using simplified assumptions in which the masonry substrate is treated as a homogeneous material and the interface response is represented by simplified bond-slip relationships [7]. Although such approaches can reproduce the global response with reasonable accuracy, they often neglect the heterogeneous nature of masonry and the local effects induced by mortar joints [12]. However, masonry is inherently composed of

brick units and mortar joints with significantly different mechanical properties, and experimental evidence has shown that mortar joints frequently act as weak regions where stress concentrations, crack initiation, and damage localization occur preferentially [9], [11].

Recent investigations have highlighted the importance of explicitly considering mortar joints in the modelling of FRP-strengthened masonry systems. Ghiassi et al. [10] demonstrated that mortar joints considerably influence local interface stresses, crack propagation, and global force-slip behaviour. Similarly, Sassoni et al. [12] reported that mortar joints and brick surface characteristics significantly affect the measured debonding force and may lead to inaccuracies when neglected in theoretical predictions. Nevertheless, despite these findings, only limited research has explicitly investigated the influence of mortar joint discontinuities on interfacial stress transfer, damage evolution, and effective bond length.

Another important limitation in existing studies concerns the modelling strategies adopted for simulating the debonding process. Many numerical investigations employ simplified interface laws based on cohesive elements or bond-slip relationships without fully considering the interaction between interface degradation and masonry bulk damage [7], [11]. However, experimental observations indicate that the debonding phenomenon is strongly coupled with crack propagation within both mortar joints and masonry units. Therefore, simplified interface-only approaches may not accurately reproduce the actual failure mechanisms occurring in FRP-strengthened masonry systems.

In addition, although several studies have successfully employed two-dimensional numerical approaches to investigate FRP-to-masonry bond behaviour, important aspects related to local stress redistribution near mortar joint discontinuities remain insufficiently understood [10], [11]. Furthermore, limited research is available regarding the parametric influence of masonry heterogeneity on bond performance, particularly concerning mortar joint thickness, mortar-to-brick elastic modulus ratio, reinforcement length, and interface properties.

Based on these observations, the main research gap identified in the literature is the limited understanding of how mortar joint discontinuities influence the local and global behaviour of FRP-to-masonry bonded systems. Existing approaches still provide insufficient information regarding the interaction between masonry heterogeneity, interface damage, crack propagation, and effective bond length evolution. Therefore, further research is required to

develop more realistic numerical and analytical approaches capable of accurately representing the debonding mechanisms in FRP-strengthened masonry structures.

1.3. Aim and Objectives

The main aim of this research is to numerically and analytically investigate the bond behaviour between Fiber Reinforced Polymer (FRP) composites and masonry substrates while considering the influence of mortar joint discontinuities. The study focuses on understanding how the heterogeneous nature of masonry affects interfacial stress transfer, damage evolution, and effective bond length in FRP-strengthened masonry systems.

To achieve this aim, the following objectives are defined:

- Develop a nonlinear finite element model capable of simulating FRP-to-masonry bond behaviour under monotonic loading conditions.
- Define appropriate constitutive models for brick units, mortar joints, and FRP-masonry interfaces using nonlinear material behaviour and cohesive interaction laws.
- Investigate the influence of mortar joint discontinuities on stress transfer mechanisms, crack initiation, and debonding propagation.
- Perform a parametric sensitivity analysis considering mortar joint thickness, reinforcement length, and mechanical properties of masonry constituents.
- Analyse the evolution of effective bond length along heterogeneous masonry substrates.
- Compare the numerical response with available experimental and analytical results reported in the literature.

1.3.1. Scope and Limitations

The present research focuses on the numerical and analytical investigation of FRP-to-masonry bond behaviour using a two-dimensional nonlinear finite element modelling approach. The study primarily considers externally bonded FRP systems subjected to

monotonic loading conditions representative of single-lap shear tests commonly adopted in the literature.

Brick units and mortar joints are modelled separately in order to account for the heterogeneous nature of masonry and the local effects induced by mortar joint discontinuities. The FRP-to-masonry interface is represented using cohesive interaction laws capable of simulating damage initiation and progressive debonding behaviour.

The investigation includes the influence of mortar joint thickness, mortar-to-brick elastic modulus ratio, reinforcement length, and interface properties on stress transfer mechanisms and effective bond length evolution. However, the study is limited to two-dimensional numerical analyses and does not explicitly consider cyclic loading, environmental degradation, temperature effects, or long-term behaviour.

1.3.2. Significance of the Study

The bond behaviour between FRP reinforcement and masonry substrates plays an important role in determining the effectiveness of strengthening systems used for masonry rehabilitation. Premature debonding at the FRP-masonry interface frequently limits the full utilization of the reinforcement capacity and may lead to brittle failure mechanisms [11], [12]. Therefore, improving the understanding of interfacial stress transfer and debonding behaviour is essential for the development of reliable strengthening strategies.

The significance of the present study lies in its explicit consideration of mortar joint discontinuities within the numerical and analytical investigation of FRP-to-masonry bond behaviour. Unlike many existing studies that idealize masonry as a homogeneous material, the present work considers the heterogeneous composition of masonry and investigates how local discontinuities influence stress redistribution, damage propagation, and effective bond length.

Furthermore, the study contributes toward improving nonlinear modelling strategies for FRP-strengthened masonry systems and may support the development of more realistic analytical interpretations and design-oriented approaches for masonry strengthening applications.

1.4. Structure of the Dissertation

This dissertation is organized into five chapters addressing the numerical and analytical investigation of FRP-to-masonry bond behaviour considering mortar joint discontinuities.

Chapter 1 presents the general background of FRP strengthening systems for masonry structures, the research motivation, and the main research gap identified in the literature. The chapter also defines the objectives, scope, limitations, and significance of the present study.

Chapter 2 provides a comprehensive literature review on FRP-strengthened masonry systems, focusing on FRP-to-masonry bond behaviour, debonding mechanisms, bond-slip relationships, effective bond length, and the influence of mortar joint discontinuities. Numerical modelling approaches, cohesive interface formulations, and analytical models available in the literature are also reviewed.

Chapter 3 describes the numerical and analytical methodology adopted in this research. The chapter presents the constitutive modelling of masonry materials and FRP interfaces, the finite element modelling strategy developed in ABAQUS, the boundary conditions, meshing procedures, and the cohesive interaction laws used to simulate the debonding process. The parameters considered in the sensitivity analysis are also introduced.

Chapter 4 presents and discusses the numerical results obtained from the nonlinear simulations. The influence of mortar joint discontinuities on stress transfer, interface damage evolution, and effective bond length is analysed. The effect of key geometric and mechanical parameters on the global and local bond behaviour is also evaluated and compared with findings reported in the literature.

Finally, Chapter 5 summarizes the main conclusions of the research and highlights the principal findings related to FRP-to-masonry bond behaviour considering masonry heterogeneity. Recommendations for future research and possible extensions of the present work are also presented.

THIS PAGE WAS INTENTIONALLY LEFT BLANK

2. LITERATURE REVIEW

2.1. Masonry structures and strengthening techniques

For centuries masonry structures have been a prevailing building technology and are still used today in many constructions, especially in historical and heritage constructions [13]. The primary reasons for using masonry structures were the material availability, durability, thermal characteristics, and relative ease of construction. Nevertheless, masonry structure exhibits low tensile strength and ductility, making it vulnerable to seismic loads, environmental deterioration, and growing service loads [2], [14].

Masonry's mechanical behaviour is heavily influenced by its heterogeneous character. Masonry members are made of units (stones or bricks) bonded together with a mortar. Since each element has unique mechanical properties and the mortar joints can be considered weaker areas, these joints are significant in the initiation and propagation of cracks [8], [12]. Typical failure mechanisms in unreinforced masonry structures include diagonal tension cracking, sliding along mortar joints, and out-of-plane failure [14], [15].

Over the years many strengthening methods for existing masonry structures have been proposed to improve the performance of the structure [13]. These traditional techniques include concrete jacketing, steel bracing and steel plate bonding. These can increase both stiffness and strength [13] but also add load to the structure, can be prone to corrosion and are complex to install. Additionally, these methods will significantly alter the geometry of the structure [13], [16].

Fiber Reinforced Polymer (FRP) composites have gained more interest over the past years as a means to strengthen masonry structures. These systems generally consist of fibers in a polymer matrix and the most popular types include Carbon Fiber Reinforced Polymer (CFRP), Glass Fiber Reinforced Polymer (GFRP) and Aramid Fiber Reinforced Polymer (AFRP). Advantages of FRP composites are high strength, low weight, corrosion resistance and simple installation which are useful in rehabilitation applications where invasiveness must be minimized [2], [13].

Many different ways of applying FRP for strengthening masonry have been developed such as external bond strengthening, internal bar or strip application, wrapping and textile reinforcement [16], [17]. Typical FRP strip strengthening configurations adopted for masonry rehabilitation are illustrated in Figure 2.1. In the context of FRP strengthening the externally bonded method is perhaps the most common application because it is easy to install and enhances both the flexural and shear capacity of the masonry member [13].



(a) Diagonal FRP strip configuration (b) X-shaped FRP strip configuration(c) FRP strips with connectors

Figure 2.1: Different FRP strip strengthening configurations used in masonry rehabilitation [13].

It has been demonstrated in the past by various research studies that the application of FRP composites to masonry structures can significantly increase the capacity, stiffness, and ductility of members under various types of loading, both in-plane and out-of-plane [2], [15]. However, it appears that premature debonding between the FRP and the masonry substrate is often a failure mechanism, restricting the efficiency of the system [11], [12]. Because of this the behaviour of the bond between FRP and masonry has become one of the most significant topics to be studied.

2.2. FRP Composites in Masonry Rehabilitation

In recent decades, Fiber Reinforced Polymer (FRP) composite materials have become one of the widely adopted materials for rehabilitation and strengthening of masonry structures. Its increasing use in structural engineering is primarily due to its high tensile strength, low

density, corrosion resistance and simple installation over conventional strengthening techniques [13]. In masonry strengthening, FRP materials are widely utilized to enhance load carrying capacity of existing building structures that are exposed to earthquake actions, decay of construction material, and increment of design load [2], [14].

FRP composites consists of fibers or strands of the reinforcing materials embedded in a resin matrix. By fiber type, the most prevalent systems used in civil structures are Carbon Fiber Reinforced Polymer (CFRP), Glass Fiber Reinforced Polymer (GFRP) and Aramid Fiber Reinforced Polymer (AFRP) [13]. For strengthening applications, CFRP material is commonly preferred because it has high stiffness, high tensile strength and good fatigue performance. GFRP material can be selected as a relatively economic option. AFRP material has high impact resistance and energy absorption capacity [13].

The use of FRP composites for structural rehabilitation has been researched on various forms of strengthening such as flexural strengthening, shear strengthening, confinement and seismic retrofit [3], [15]. Among various techniques of applying FRP composite to masonry structures, externally bonded (EB) FRP laminate or sheets strengthening seems to be the one mostly utilized owing to its simple application procedure and its effectiveness on in-plane and out-of-plane performance of masonry elements [13]. The high-strength FRP sheets or laminates are attached to the masonry surface using epoxy resins such that shear stresses are effectively transferred between the masonry substrate and FRP materials.

A typical application of externally bonded FRP laminates on masonry walls is illustrated in Figure 2.1.



Figure 2.2: Strengthening of masonry wall using externally bonded FRP laminates [18].

Several experimental researches have demonstrated the benefits of FRP strengthening application in terms of improvement of mechanical Behaviour of masonry structures. Triantafillou [15] found that seismic resistance and ductility of masonry walls was significantly increased when reinforced using externally bonded CFRP laminates. Similarly, Ehsani et al. [2] showed that the strength and dissipated energy of FRP-retrofitted masonry walls under static lateral load simulating seismic forces is higher than unstrengthened walls. Also other studies showed that FRP application improved the stiffness, strength and durability by postponing the crack propagation [4], [5].

Another promising type of FRP reinforcement application in masonry structures is near-surface mounted (NSM) technique. FRP bars or strips are placed inside grooves cut into the surface of the masonry members and bonded to the surrounding substrate by adhesives [16], [17]. Comparing with the externally bonded system, the NSM technique could potentially improve the bond performance between reinforcement and masonry and also the reinforcement is better protected against environmental attack or mechanical damages [16].

However, there are a number of practical problems associated with FRP strengthening such as long term Behaviour and mode of failure. One of the major issues is prematurity debonding failure between masonry and FRP composite which resulted in failure to fully exploit the reinforcing capabilities of FRP composites [11], [12]. The bond Behaviour between FRP composites and masonry masonry is sensitive to the composite material characteristics, interfacial properties, the roughness of the masonry surface and the presence of mortar joints [12]. Hence, the investigation of FRP composites interaction with heterogeneous masonry substrate becomes very important in order to develop appropriate and effective strengthening strategies and numerical modeling approaches.

2.3. Bond Behaviour of FRP-to-Masonry Systems

The Behaviour of FRP strengthening systems on masonry relies primarily on the quality of the bond between the FRP reinforcement and the masonry. This bond mechanism is responsible for transmitting loads from the masonry element to the FRP reinforcement thus allowing the FRP strengthening system to carry its part of the global loads. Therefore the

bond mechanism is largely influential in controlling the load carrying capacity, stiffness, ductility and the failure modes of FRP-strengthened masonry structures. Experimental and numerical analyses conducted have revealed that an insufficient bond performance will result in a premature debonding failure occurring before the FRP reinforcement has achieved its tensile capacity [10], [11].

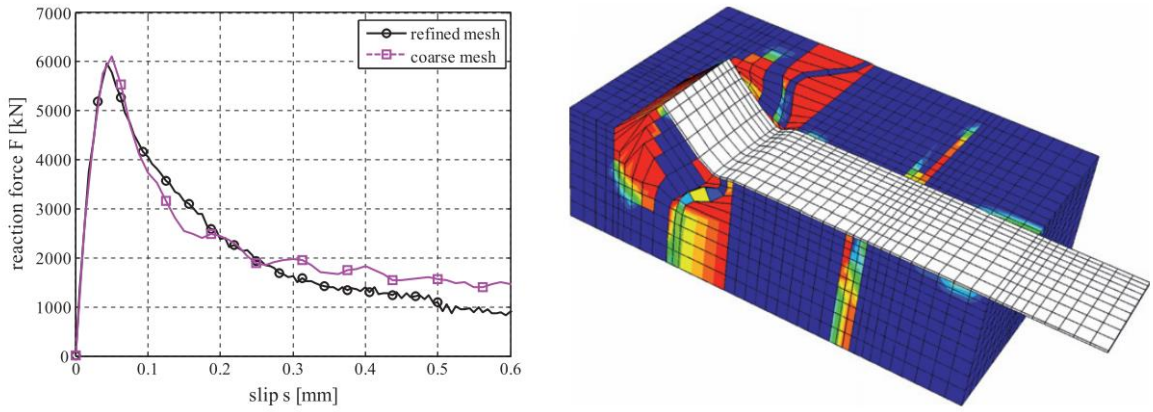


Figure 2.3: Numerical simulation of debonding propagation and stress concentration in FRP-strengthened masonry systems [11].

In FRP-to-masonry systems the bond mechanism is developed through the interaction between the masonry substrate, the adhesive layer, and the FRP reinforcement. In general terms stresses will be transferred across the interface mainly by means of interfacial shear stresses with normal stresses that might develop due to geometric discontinuities, crack opening or local deformational effects [14], [19]. Typical debonding and cracking failure modes observed in FRP-strengthened masonry systems are illustrated in Figure 2.3 [14]. These stresses are normally more concentrated on the loaded end of the bonded zone, where debonding normally initiates [10], and with increased load, this phenomenon will propagate along the length of the bonded region, reducing the effectiveness of the stress transfer mechanism.

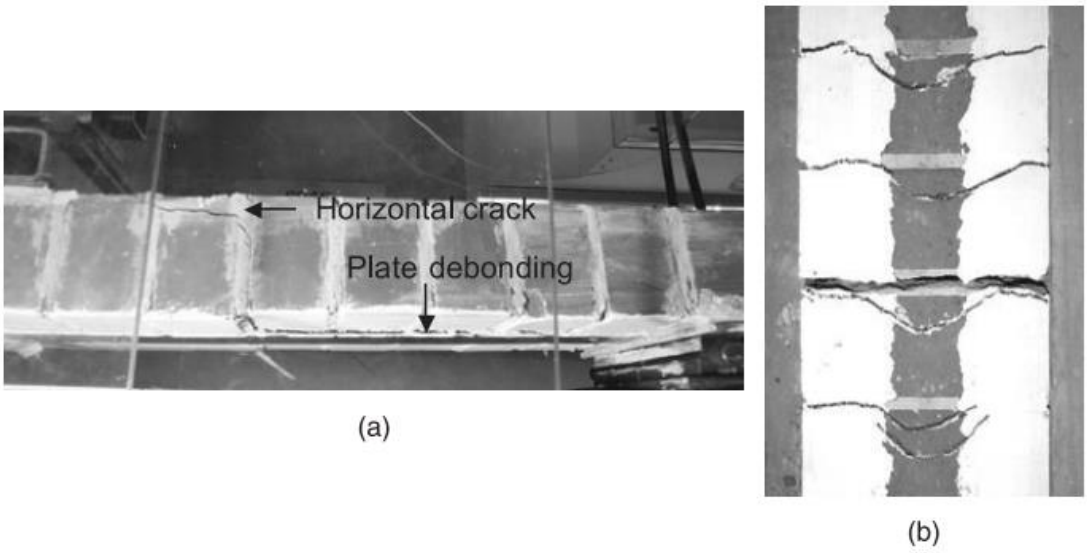


Figure 2.4: Typical failure modes in FRP-strengthened masonry systems: (a) flexural-shear debonding failure and (b) shear failure [14].

The experimental evidence obtained so far has indicated that the debonding failure of FRP on masonry typically occurs in a thin layer of the masonry substrate instead of in the adhesive interface [11], [12]. Substrate debonding is often referred to as one of the dominant failure modes of FRP externally bonded to concrete and masonry. This type of failure is attributed to the brittle nature of masonry and the relatively high modulus of the FRP composite that causes stress concentrations around the FRP/adhesive interface [9], [11]. The high concentrations are sufficient to propagate cracks into the masonry substrate and hence debonding.

FRP-masonry bond-slip relationships that describe the relationship between interfacial shear stresses and the sliding displacements of the interface between FRP and masonry are generally used to represent the bond performance [10], [14]. The bond slip curve initially displays a near linear-elastic Behaviour followed by a post-peak softening Behaviour related to continued crack growth along the interface. The area under the bond-slip curve corresponds to the fracture energy of the interface and is related to the energy required for propagating debonding [11].

The bond Behaviour between FRP and masonry has been analyzed experimentally and numerically by a number of researchers. A finite element model for NSM FRP strengthened walls was developed by Petersen et al. [17], where the FRP-to-masonry interface interaction

was described using interface elements governed by local bond slip constitutive relationships derived from pull tests. They demonstrated that the interface behaviour has a major impact on the load redistribution and the global performance of strengthened masonry walls. Similarly Xia and Oehlers [10] used an interface based numerical model which has been able to capture progression of debonding using tangential and normal interface constitutive relations.

Advanced numerical analyses have also addressed the influence of masonry heterogeneity on local interface stresses and propagation of failure. Fedele and Milani [20] simulated the delamination of FRP from masonry using fully 3D FE models and showed how the crack propagation into the masonry is a fully 3D process that is highly sensitive to the ratio of FRP width and masonry width. The mortar joints also proved to act as crack propagation paths, and the cracks spread along and to the sides of the bonded area. They concluded that by increasing the FRP width the overall ductility decreases, whereas the localized stresses near the anchorage zones increase.

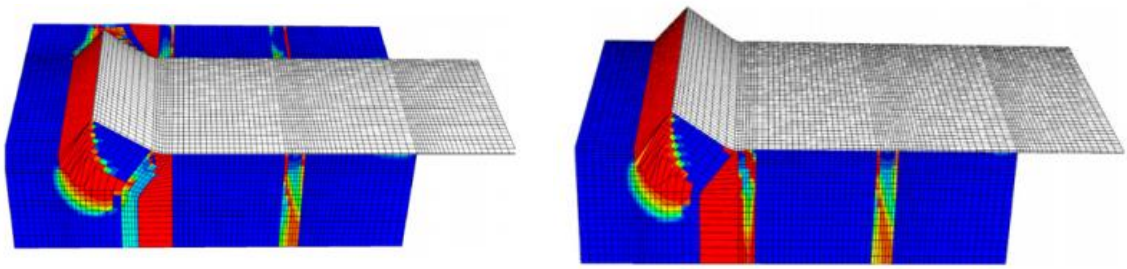


Figure 2.5: FE simulation of FRP delamination from masonry for different FRP width-to-masonry width ratios: (a) narrow FRP strip and (b) wide FRP strip [20].

Several parameters that influence the bond performance of FRP strengthened masonry systems have been identified; among these include masonry material properties, mortar joint characteristics, adhesive stiffness, FRP stiffness, bonded length, surface preparation condition etc. [11], [12]. Among the most important parameters are the mortar joints as these represent weaknesses in stiffness and strength, and localized stress concentration near and through these joints causes cracking within the masonry substrate [12].

An additional parameter related to bond performance is the effective bond length of the reinforcement. From experiments it has been revealed that after a certain anchorage length increasing it has no benefit for increasing the transferrable load [7], [11]. This can be attributed to the stress transfer that normally occurs in a small localized zone at the loaded end of the reinforcement. Therefore the effective bond length must be calculated accurately to ensure that strengthening occurs efficiently and failure by premature debonding does not occur.

Despite considerable effort many problems of FRP-to-masonry bond performance are not well understood, especially regarding the effect of the non-homogeneity of masonry and mortar joints on local interface stress states and failure propagation [12], [20]. Many numerical models assume masonry properties to be homogeneous and this leads to failure to correctly predict how local interface stresses propagate through the concrete due to cracking. Thus, further work in analysis, numerical modeling and experiment is necessary to capture the interaction between local interface failure mechanisms and the global Behaviour of the composite structure.

2.4. Failure Mechanisms and Debonding Phenomena

Bond between the FRP reinforcement and the masonry substrate is a critical factor controlling the effectiveness of FRP strengthening systems on masonry structures. Even though FRP composite exhibits excellent tensile strength and stiffness, the failure modes of strengthened masonry member could be induced by debonding phenomenon before FRP material reaching its ultimate tensile strength [11], [12]. Typical debonding behaviour and crack propagation observed in FRP-strengthened masonry specimens are illustrated in Figure 2.6 [11]. Hence, knowledge on the various modes of failure related to FRP-to-masonry systems is necessary for effective design and assessment of strengthening works.

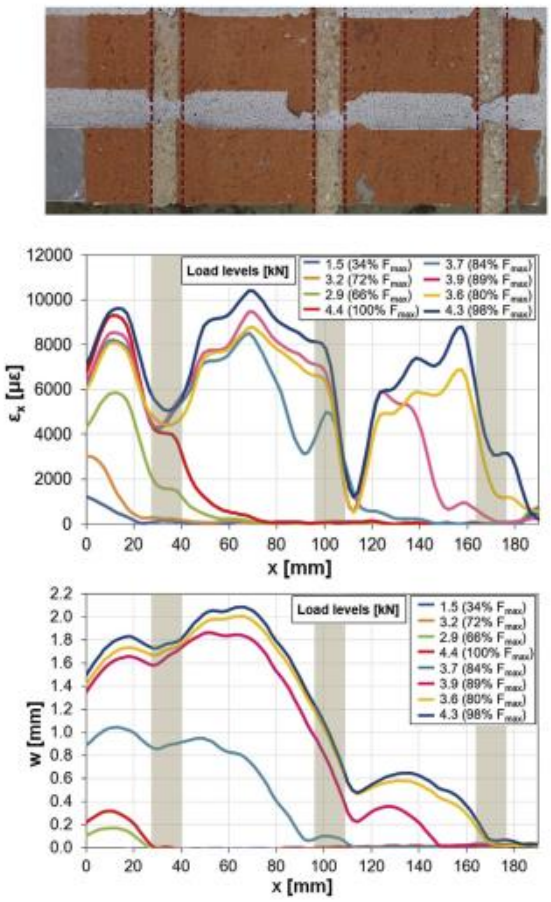
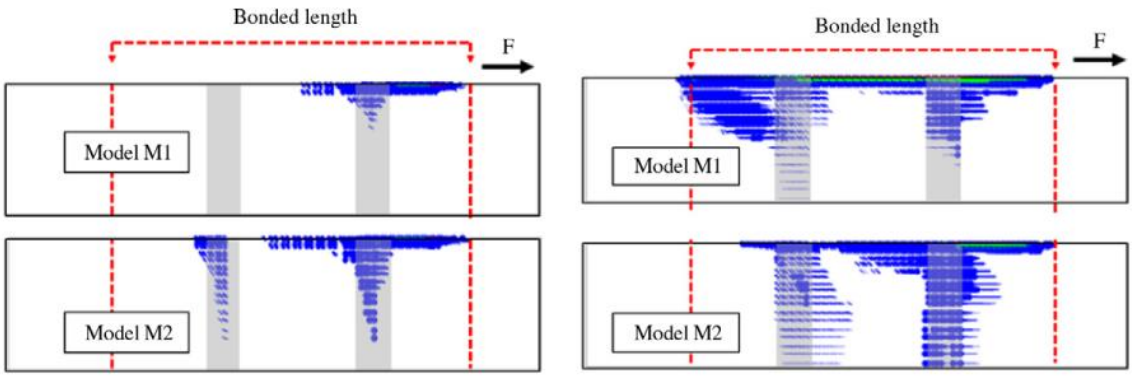


Figure 2.6: Debonding test results for a representative masonry specimen showing the failure mode and the distributions of longitudinal strain and displacement along the bonded interface at different load levels [11].

Experimental evidences have showed that several failure modes might be developed in FRP strengthened masonry structures, varying from mechanical property of masonry substrate, adhesive, fiber-optic system and external load [6], [14]. Failure modes of FRP-to-masonry can include FRP rupture, cohesive failure, adhesive failure, substrate failure and mixed-mode failure involving shear and normal stress along interface. The most dominant failure mechanism of FRP-to-masonry systems with externally bonded FRP strips is the failure due to the mortar/substrate cracking within the layer of substrate right beneath the adhesive layer [9], [12]. Figure 2.7 shows the crack distribution and debonding propagation patterns for different FRP width-to-masonry width ratios [9].



(a) FRP width-to-masonry width ratios r=0.42 (b) FRP width-to-masonry width ratios r=0.9

Figure 2.7: Crack distribution and debonding propagation in FRP-strengthened masonry specimens for different FRP width-to-masonry width ratios

The initiation of failure of FRP-to-masonry member under applied load is usually attributed to stress concentration at the loaded end, where the maximum interfacial shear stress and peeling stress develop [10], [14]. Once the damage initiates through cracking of mortar joints or within masonry substrates in shallow depths near the adhesive interface, the load transfer between the FRP reinforcement and the masonry substrate progressively deteriorates [11]. Eventually the debonding crack will propagate along the bonded interface and a portion of the FRP reinforcement will debond from the substrate.

The mechanical behaviour of masonry influences significantly on the mechanism of crack initiation and propagation during the debonding process. As masonry is a composite material comprising discrete brick elements and mortar joints, the interfacial stress concentration develops particularly at the interfaces of mortar joints where the stiffness and tensile strength of mortar is typically lower than brick units [10], [12]. Experimental results show that the cracks propagate easily along the mortar joints, and distribute unevenly at the bond interface [9]. Ignoring the discrete nature of masonry in the analysis might lead to inaccurate results of the failure modes and debonding resistance.

There are several studies carried out on the effects of geometrical and mechanical parameters to the debonding phenomenon. Fully three-dimensional finite element simulations performed by Fedele and Milani [20] proved that the failure crack propagation in the masonry substrates is highly sensitive to the ratio between FRP width and masonry width. The numerical results illustrated that when FRP strips of increased width are used,

the global ductility of the strengthened member will decrease, but stresses in certain region, near the anchorage for example, are increased. Ghiassi et al. [10] investigated the influences of arrangement and material properties of mortar joints on stress transfer mechanism and cracks propagation, which illustrated a significant dependence of the phenomena on the characteristics of the mortar joints.

The bonded length of the FRP reinforcement is also crucial on controlling the failure mechanism. It was found from experimental results that the load transfer primarily takes place within a region of limited length close to the end of reinforcement, which can be called as effective bond length [7], [11]. As the bonded length increases beyond the effective bond length, the increase in load transfer capacity would be limited as the distribution of stresses becomes more concentrated near the anchorage. Therefore, debonding could be induced even if the length is sufficiently long.

Based on various numerical modelling techniques such as cohesive zone models, interface elements and traction-separation laws for interface, attempts have been made to reproduce and analyse the failure mechanisms of FRP-to-masonry members [19], [17]. Good agreement has been shown between numerical prediction and experimental outcome with regard to initiation of cracks, damage propagation and load-displacement curves. However, accurate representation of interaction among masonry heterogeneity, mortar joints and interface degradation remain an open research area.

2.5. Experimental Single-Lap Shear Tests

The most commonly adopted methods to experimentally characterize the local bond response of composite strengthening systems on masonry structures are the single-lap shear tests. Single-lap shear tests provide relevant information about the progression of strains in the reinforcement, load transfer capacity of the bonded interface, and progression of local damage mechanisms with applied loading [22].

The test consists of an externally strengthened masonry prism by a bonded FRP or FRCM strip and a tensile loading applied. Relative displacement between the reinforcement and the substrate, as well as the strain distribution along the bonded length are recorded during

the test. Figure 2.8 shows a schematic view of typical single-lap shear test arrangement for masonry specimens.



Figure 2.8: Experimental setup of a single-lap shear test for investigating the bond behaviour between composite reinforcement and masonry substrate [22].

Recently the effect of the substrate geometry and interface constitutive behaviour on the response of strengthened masonry structures gained a lot of attention. The effect of curvature on single-lap shear test of FRCM strengthened masonry has been investigated in Grande et al. [22]. The experiments performed on flat and curved masonry specimens demonstrated the high influence of curvature on the local stress transfer and debonding process. Their numerical analyses showed the interaction between the normal and tangential stresses at the reinforcement-matrix interface to be of primary importance in the case of curved substrates at either the intrados or the extrados side.

Further detailed simulations of single-lap shear test were performed by Dimitri et al. [21] who developed a cohesive zone modelling, coupled to concrete damage plasticity, to analyse the nonlinear response of CRM system. Their study points out that the debonding behaviour is strongly influenced by the constitutive formulation for the mortar matrix and by the interaction between mortar cracking and interface deterioration.

Experimental investigations on CRM-reinforced masonry panels subjected to cyclic shear-compression loading were also carried out in recent studies. The results demonstrated that CRM reinforcement can significantly improve the shear resistance, ductility and crack distribution of masonry panels while modifying the failure mechanisms under cyclic loading conditions [24].



Figure 2.9: Experimental setup of a bond test performed on a strengthened masonry specimen during single-lap shear loading [24].

Some experimental works have also looked at the influence of the reinforcement shape and the geometry of the substrate on the bond behaviour of masonry structures. Grande and Milani [23] have also developed analytical models for FRP-strengthened curved masonry specimens. Bertolesi et al. [27] has also developed micro-mechanical FE models, to explain the local damage behaviour under single-lap shear tests on curved masonry pillars.

It has been shown from all these experimental studies that many parameters that strongly affect the bond response exist: the mechanical properties of the masonry, the arrangement of mortar joints, the stiffness of the reinforcement, the bonded length, and the interface constitutive behaviour [10], [12], [25]. Due to their interaction, single-lap shear test seems to be the main way for the calibration and validation of the analytic or numeric bond slip models for FRP strengthened masonry.

2.6. Interface Modelling and Bond-Slip Behaviour

One of the major difficulties encountered in the analysis of strengthened masonry systems is the accurate description of the FRP to masonry interface. The structural response is largely dominated by the local mechanisms of stress transfer at the bonded interface and therefore various analytical and constitutive models are presented to represent the stress-slip relationship between the reinforcement and masonry substrate [19], [21].

In general, the bond-slip relationship is described through constitutive laws, which describe the shear stress at the interface against the relative displacement between the substrate and the reinforcement. These laws are of great importance to predict the mechanisms of stress transfer, the progression of cracks and evolution of debonding in strengthened masonry. Various forms of constitutive laws are discussed in the literature, for example linear, bilinear, exponential and multilinear traction-separation laws [11], [21]. Among the constitutive relationships, bilinear constitutive laws are most commonly employed to describe the Behaviour of interface between masonry and FRP reinforcement as they are capable of describing both the linear and post peak Behaviour of the interface response.

Cohesive zone models have become extensively used to describe the Behaviour of the FRP interfaces, which rely on the application of traction separation constitutive laws describing stiffness parameters, strength and fracture energy of interface [21]. The criteria for initiation and propagation of damages at interface are usually based on stresses, while the degradation of interface is often characterized by the progressive softening of stiffness related to the cracking of the bond along the interface.

Studies by researchers in recent years have clearly demonstrated that interface response is not only dictated by shearing actions but by combination of normal and shear forces. Grande et al. [22] showed that local Behaviour of debonding at curved masonry substrates retrofitted with FRCM systems are severely influenced by normal and shear stress interactions. The local mechanisms of debonding are reported to be strongly affected by mixed mode fracture conditions especially around sharp variations of geometry and stress concentration regions. Figure 2.12 illustrates a typical interface constitutive law adopted to represent the nonlinear bond-slip behaviour and residual stress transfer mechanisms of FRP/FRCM interfaces [22].

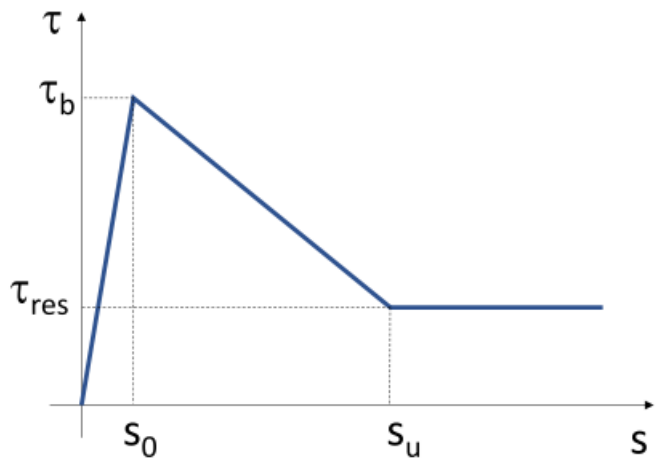


Figure 2.10: Schematic representation of the interface constitutive law used for modelling the nonlinear bond-slip behaviour of FRP interfaces [22].

Constitutive Behaviour of mortar matrix is an additional significant factor to be considered during numerical simulation of bond-slip response. Dimitri et al. [21] investigated the different mortar constitutive laws and conclude that polynomial and exponential damage models had the most significant impact on crack propagation and interface degradation in the context of single lap shear test. The mortar cracking is therefore of critical importance in describing experimental results of debonding Behaviour.

The concept of effective bond length for FRP-to-masonry connection is of critical importance. Several analytical and numerical models show that beyond the loaded end, only a portion of the bond interface is engaged in transferring stresses and thus the anchorage length does not continuously increase load transferable for length greater than a particular value [7], [11]. Hence, effective bond length is often used in analytical formulations of strengthened masonry systems with FRP reinforcement.

Various analytical and closed-form models are available in the literature to predict bond strength and mechanism of stress transfer at FRP to masonry interface. An interphase model by Freddi and Sacco [19] describes the nonlinear Behaviour between masonry and FRP using interface constitutive Behaviour determined from experimental data. Furthermore, the development of data-driven models for predicting the bond strength of FRP strips bonded to masonry substrates is introduced by Kamgar et al. [26], in which artificial neural network and regression techniques based on experimental database obtained from pull out tests are used to predict the bond strength. Figure 2.13 compares the predictive capability of different

machine learning models with existing analytical formulations for estimating the bond strength of FRP-to-masonry systems [26].

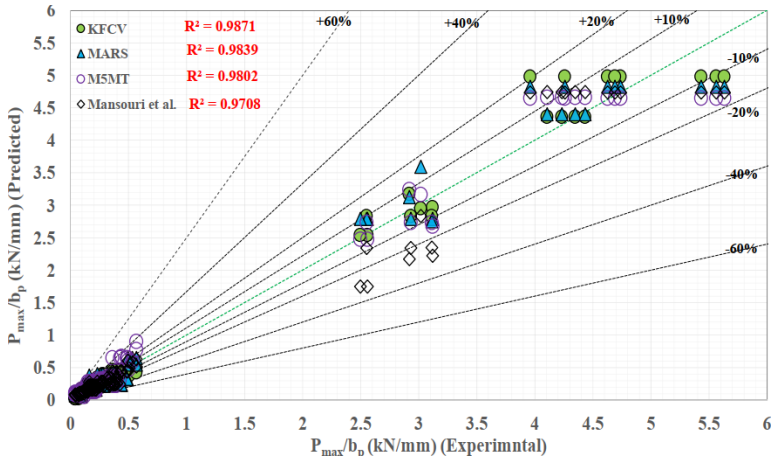


Figure 2.11: Comparison between experimental and predicted bond strength values using different machine learning and regression models for FRP-to-masonry bond behaviour prediction [26].

Despite the continuous advances in modeling FRP to masonry bond Behaviour, numerous parameters, such as effects of discontinuities in mortar joints, irregularities of masonry substrate and local stress state at interface, are yet difficult to be modeled and predicted effectively [12], [19], [22].

2.7. Numerical Modelling of FRP-to-Masonry Bond Behaviour

The local mechanisms of interaction between FRP systems and masonry substrates can be investigated by various numerical modelling techniques. They help to better characterize the stress transfer and crack propagation and to provide information about the development of the damage at the interface which are difficult to measure experimentally. The use of finite element models is also a very effective way to study the influence of materials parameters, the arrangement of reinforcement geometry and the distribution of mortar joints on the overall bond response of FRP strengthened masonry systems [7], [10].

Several modeling strategies have been proposed, depending on the level of detail needed for the study of interaction mechanisms: simple macro-models consider masonry as a homogeneous material and micro-mechanical approaches analyze each masonry component

separately (brick, mortar joints, interface layer) [27]. Macro-models have the advantage of being less time consuming but they are less suitable for modeling local stress concentrations and cracks developed due to mortar joints discontinuities.

Freddi and Sacco [19] propose an interphase model capable to reproduce the interaction between masonry substrate and reinforcement through a interface constitutive law. It allowed to reproduce the degradation of the interface and stress redistribution, while simplified perfect bond approaches are too idealistic.

The influence of mortar joints on the local response was studied numerically by Ghiassi et al. [10]. It was shown that the relative position of the mortar joints can have a significant influence on the interfacial stress distribution and the location of the crack initiation. Local concentrations of stresses near mortar joint discontinuities led to a non-uniform progression of cracks along the interface.

For curved masonry geometry, some advanced numerical simulations have also been performed. Grande and Milani [23] proposed numerical formulations for curved masonry specimens loaded with a single lap-shear test, in which it was shown that the curvature of the masonry specimen affect the stress transfer mechanism at the interface. Bertolesi et al. [27] developed detailed micro-mechanical FE models for FRP strengthened curved masonry pillars and accurately reproduced local damage mechanisms and debonding Behaviour observed experimentally. Figure 2.14 presents the finite element modelling strategy and boundary conditions adopted for curved masonry specimens subjected to single-lap shear loading [27].

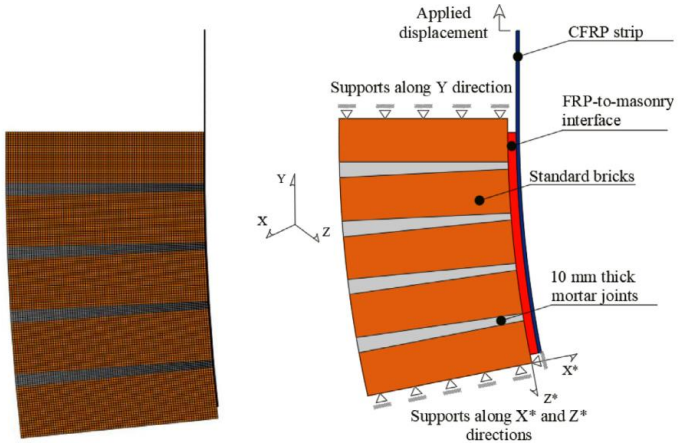


Figure 2.12: Micro-mechanical finite element model and boundary conditions for FRP-strengthened curved masonry specimens subjected to single-lap shear tests [27].

A recent numerical approach is based on the use of cohesive interface elements together with a constitutive law for the masonry Behaviour. Dimitri et al. [21] used this modeling strategy for CRM and demonstrate that the phenomena of mortar cracking and interface damage are highly related during the crack propagation in debonding.

In summary, numerical modeling techniques have become indispensable for the analysis of local mechanisms of interaction between FRP reinforcement systems and masonry substrates, even though predicting the accurate Behaviour of local debonding remains a challenge due to the non-linear response of masonry and interface variability [10], [19], [27].

2.8. Research Gaps and Objectives of the Present Study

Over the past decades, significant research effort has been directed toward understanding the bond Behaviour of FRP/FRCM strengthening systems applied to masonry substrates. The results of experimental tests, analytical derivations and numerical simulations have greatly contributed to clarify the stress transfer mechanisms, debonding progression and constitutive laws at the interface. Nevertheless, several issues regarding local interaction between composite reinforcements and heterogenous masonry substrates are yet not well understood.

Many analytical and numerical solutions found in the literature simulate masonry as an equivalent homogenous material with proper overall mechanical properties. Despite the fact that these approaches can simplify the modeling, and decrease computational effort, they do not seem able to capture the local stress concentrations and crack propagation mechanisms due to mortar joints irregularities. Experimental results and sophisticated numerical analysis clearly indicate that the Behaviour of the mortar joints plays a crucial role in the initiation and development of the interface failure mechanisms, particularly close to locations where stress concentration and geometric discontinuity are located [10], [12], [22]. However, the interaction between the arrangement of mortar joints and local interfacial stress redistribution is not completely clarified yet.

The second problem encountered in the literature refers to the constitutive modelling of FRP to masonry interface. Even though cohesive zone modelling and traction-separation relationships were adopted widely to model the interface Behaviour, it is still quite difficult to calibrate the parameters of the interface constitutive model when the masonry is

characterized by a heterogenous response due to the variability of the masonry material, of mortar properties and of failure mechanisms [19], [21]. Furthermore, the interaction between cracking of the masonry substrate and interface degradation is generally simplified, and then the experimental debonding Behaviour is not always replicated accurately.

More recently, numerical works have pointed out the importance of local mixed-mode stress state and the contribution of substrate geometry on the bond response of strengthened masonry structures [22], [23], [27]. However, still more research is needed to improve the understanding on the mechanism of stress transfer to local level and the development of the propagation of cracking and the effective bond length, in presence of mortar joint discontinuities.

Based on the aforementioned considerations, the purpose of the present study is to perform numerical investigation on the bond Behaviour of FRP reinforcement to masonry substrate using Finite Element Model approach. The main focus is to reveal the effect of mortar joint discontinuities on the local interface response and debonding mechanisms and to investigate the interfacial stress distribution, the crack propagation pattern and the effective bond length for the strengthening system.

Furthermore, a parametric sensitivity analysis will be carried out to study the influence of the various material and interface parameters on the global and local Behaviour of the FRP-strengthened masonry structures. The findings from the present study would improve the understanding of the local phenomenon occurring at the interface due to the heterogeneity response of the masonry and contribute to the rational design of strengthened masonry elements.

THIS PAGE WAS INTENTIONALLY LEFT BLANK

3. METHODOLOGY

3.1. Overview

The procedure followed to analyse the bond behaviour between FRP reinforcements and masonry substrate is presented in this chapter. An analytical formulation combined with a finite element modeling methodology is used to study the stress transfer mechanisms, the interfacial debonding behaviour and the effect of mortar joint discontinuities on the local and global Behaviour of reinforced masonry systems.

The analytical formulation is based on the standard bond-slip theory and on the CNR design provisions for externally bonded FRP systems. It incorporates equilibrium equations, kinematic compatibilities and bond-slip constitutive laws that relate the force at the FRP reinforcement to the slip at the FRP-masonry interface. Particular emphasis is put on the interface stress transfer mechanisms, on the dissipation of the fracture energy and on the develop of effective bond length when debonding is propagating.

A finite element modeling methodology is then developed to reproduce the nonlinear Behaviour of the FRP-masonry interface. This model involves both the masonry substrate, the FRP reinforcement and a cohesive interface represented through a traction-separation relationship. This modeling strategy aims to describe the development of damage at the interface, the debonding propagation and the local stress concentration near the mortar joints.

The finite element model was validated by comparing its response (load-displacement relationship, damage evolution and debonding Behaviour) to results from numerical analyses or from experimental tests reported in literature. The obtained results allowed to investigate, using the developed FE model, through a sensitivity analysis, the effect of interface parameters, materials properties and mortar joint configuration on the bond and effective stress transfer Behaviour of FRP reinforced masonry systems.

3.2. Analytical Formulation of FRP-to-Masonry Bond Behaviour

The behaviour of externally bonded FRP strengthening systems is governed by the transfer of tensile forces from the FRP reinforcement to the masonry substrate through the bonded interface. When an external tensile force is applied to the FRP strip, interfacial shear stresses develop within the adhesive layer and progressively transfer the load to the masonry substrate. As the applied load increases, the interfacial stresses become concentrated near the loaded end, where damage initiates and subsequently propagates along the bonded interface.

The analytical framework adopted in the present study follows the formulation proposed in the CNR-DT 200 guideline for externally bonded FRP systems. This formulation is based on three fundamental components: (i) equilibrium of the FRP reinforcement, (ii) compatibility between the FRP and masonry substrate, and (iii) the constitutive bond–slip relationship describing the interface behaviour. These analytical concepts provide the theoretical basis for the cohesive interface formulation adopted in the finite element model.

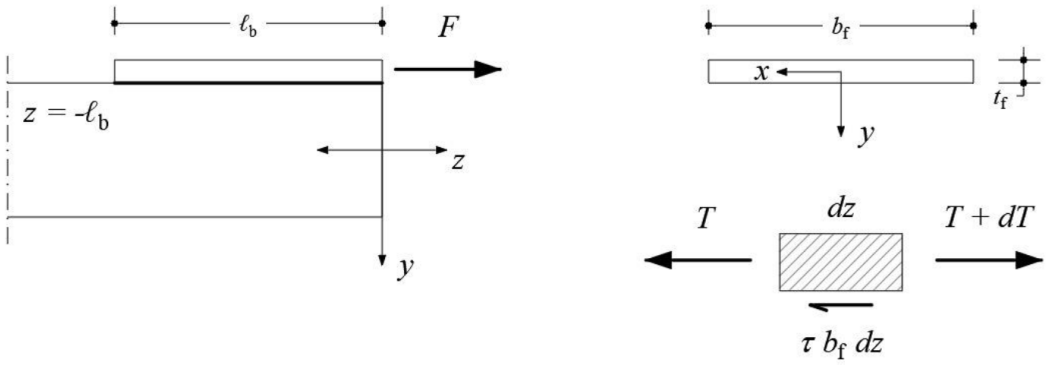


Figure 3.1: Schematic illustration of the bonded FRP-to-masonry system used for the analytical bond formulation.

3.2.1. Equilibrium and Compatibility Relationships

Figure 3.1 illustrates the bonded FRP–masonry system together with the differential element considered for the analytical formulation. The tensile force applied to the FRP reinforcement is progressively transferred to the masonry substrate through the interfacial shear stress acting along the bonded length.

The axial force carried by the FRP reinforcement is expressed as

$$T(z) = E_f b_f t_f \varepsilon_f(z) \tag{3.1}$$

Applying equilibrium to the differential FRP element yields

where τ(z) is the interfacial shear stress.

The relative displacement between the FRP reinforcement and the masonry substrate defines the local interface slip

$$s(z) = u_f(z) - u_m(z) \tag{3.2}$$

Assuming negligible deformation of the masonry substrate, the compatibility condition becomes

$$\frac{ds(z)}{dz} = \frac{T(z)}{E_f b_f t_f} \tag{3.3}$$

These equations describe the stress-transfer mechanism governing the bond behaviour and form the basis of the analytical and numerical models adopted in this study.

3.2.2. Bond-Slip Constitutive Relationships

The interaction between the FRP reinforcement and the masonry substrate is represented by the bond–slip relationship

$$\tau = \tau(s) \tag{3.4}$$

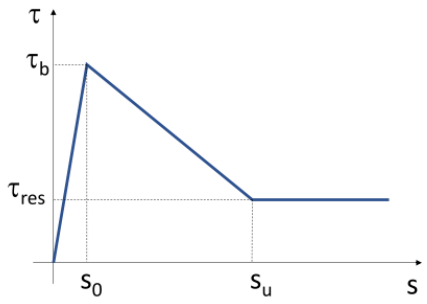


Figure 3.2: Schematic representation of bond-slip constitutive relationship and interface law

which relates the interfacial shear stress to the relative slip developed at the interface.

As illustrated in Figure 3.2, a bilinear traction–separation law is adopted to represent the interface behaviour. Initially, the interface behaves elastically according to

$$\tau = K_s s \tag{3.5}$$

where Ks is the interface shear stiffness.

When the peak bond stress τ_b is reached, damage initiates and the interface progressively softens until complete debonding occurs at the ultimate slip s_u The residual branch shown in Figure 3.2 represents the remaining shear resistance after the initiation of interface degradation.

The debonding process is governed by the interface fracture energy, defined as the area enclosed by the bond–slip relationship,

$$\Gamma_f = \int_0^{s_u} \tau(s)\ ds \tag{3.6}$$

which represents the energy required to completely separate a unit bonded area. The same traction–separation law is implemented in the cohesive interface elements of the finite element model.

3.2.3. Effective Bond Length and Debonding Resistance

According to the CNR-DT 200 guideline, the total bond force transferred through the interface is obtained by integrating the interfacial shear stress along the bonded length,

$$F = b_f \int_0^{l_b} \tau(x)\ dx \tag{3.7}$$

This relationship shows that the bond capacity depends not only on the peak interfacial stress but also on the distribution of shear stresses along the bonded interface.

The maximum transferable bond force is expressed by

$$F_{max} = b_f \sqrt{2 E_f t_f \Gamma_f} \tag{3.8}$$

indicating that the bond resistance is governed by the FRP axial stiffness and the interface fracture energy.

Because the interfacial shear stress is highly localized near the loaded end, only a limited portion of the bonded interface actively transfers the applied load. This region is referred to as the effective bond length, defined as the minimum bonded length capable of developing the maximum bond resistance. According to the CNR formulation,

$$l_e = \sqrt{\frac{\pi^2 E_f t_f}{2 f_{ctm}}} \quad (3.9)$$

where f_{ctm} is the mean tensile strength of the substrate.

The concepts of bond force, fracture energy and effective bond length constitute the principal analytical parameters employed throughout the present study to interpret the numerical results.

3.2.4. Representation of Masonry Discontinuities

The analytical formulation described above assumes a continuous bonded interface with uniform mechanical properties along the entire bonded length. In practical masonry structures, however, the bonded interface consists of alternating masonry units and mortar joints possessing different mechanical characteristics.

To account for this heterogeneous behaviour, the finite element model explicitly represents the different substrate materials by assigning independent cohesive interface properties to each interface segment according to the corresponding substrate mechanical properties. Consequently, local variations in interface stiffness, bond strength and fracture energy can be captured, enabling the influence of mortar joints on stress transfer, effective bond length and interface debonding to be systematically investigated.

Unlike the analytical formulation, which assumes a continuous stress-transfer path, the numerical model is therefore capable of representing the interruption and redistribution of interfacial stresses caused by the presence of mortar joints.

3.3. Finite Element Modelling of FRP-to-Masonry

The finite element model developed in the present study aims to reproduce the interfacial stress-transfer mechanism and debonding behaviour of externally bonded FRP reinforcement subjected to single-lap shear loading. The modelling strategy follows the heterogeneous micro-mechanical approach proposed by Bertolesi et al. [27], in which the individual masonry constituents are explicitly represented. Unlike the original study, which

considered curved masonry substrates, the present work focuses on flat masonry specimens and therefore neglects curvature effects.

The numerical analyses were performed using the commercial finite element software Abaqus. The masonry substrate was modelled explicitly by representing the masonry units and mortar joints as independent materials, allowing the heterogeneous nature of masonry to be incorporated into the numerical model. The FRP reinforcement was modelled as a linear elastic material, whereas the bond between the FRP and the masonry substrate was represented using a cohesive interface formulation governed by a bilinear traction–separation law.

Particular emphasis was placed on accurately modelling the bonded interface, since it governs the initiation and propagation of interfacial debonding. Different cohesive interface properties were assigned according to the substrate material beneath the FRP, enabling the mechanical characteristics of brick, stone and mortar joints to be represented individually. This modelling strategy allows the numerical model to capture the interruption and redistribution of interfacial stresses caused by the presence of mortar joints, which constitutes the primary objective of the present investigation.

The analyses were conducted under displacement-controlled loading to reproduce the experimental single-lap shear tests. Following calibration against the available experimental results, the validated numerical model was employed to investigate the influence of FRP axial stiffness, substrate type, mortar thickness and bond length on the stress-transfer mechanism, effective bond length and debonding behaviour of FRP-strengthened masonry systems.

3.3.1. Geometry and Model Configuration

The finite element model developed in the present study reproduces the single-lap shear test configuration commonly adopted for investigating the bond behaviour of externally bonded FRP systems on masonry substrates. A two-dimensional plane strain formulation was adopted throughout the numerical analyses. Two reference models were developed corresponding to the experimental specimens constructed using red brick and tuff stone masonry, respectively. For both models, a 10 mm mortar joint thickness was adopted during

the validation stage, while additional mortar thicknesses were introduced later in the parametric study presented in Chapter 4.

The masonry substrate was explicitly modelled by representing the masonry units and mortar joints as separate regions, allowing the heterogeneous nature of masonry to be incorporated into the numerical model. The FRP strip was externally bonded to the substrate surface, while unbonded regions of 15 mm at the lower end and 40 mm at the upper end were introduced to reproduce the experimental loading configuration, resulting in a bonded length of 330 mm for the reference validation models.

The geometrical properties of the reference brick and stone models are summarized in Table 3.1.

Table 3.1: Geometrical properties of the finite element model.

Component	Brick Model		Stone Model	
	Height (mm)	Length (mm)	Height (mm)	Length (mm)
Masonry substrate	365	250	590	380
Brick	65	250	110	380
Mortar	10	250	10	380
FRP strip	385	100	630	100
FRP bonded region	330	100	330	100

Since a two-dimensional plane strain formulation was adopted, the numerical model represents a unit thickness in the out-of-plane direction. Therefore, the reaction forces obtained from the analyses (N/mm) were multiplied by the specimen width (100 mm), corresponding to the bonded width of the FRP strip, to obtain the total bond force (N) for comparison with the reference results. The physical thickness of the FRP reinforcement is 0.165 mm for both models.

The interaction between the FRP strip and the masonry substrate was represented using a surface-based cohesive interface formulation along the bonded region. Displacement-controlled loading was applied through a reference point coupled to the free end of the FRP strip, while appropriate boundary conditions were imposed to prevent rigid body motion and accurately reproduce the experimental single-lap shear test configuration. The

constitutive material models and cohesive interface formulation adopted in the numerical analyses are presented in the following sections.

3.3.2. Constitutive Modelling of Masonry and FRP Materials

The finite element model consists of three principal components: the masonry substrate, the FRP reinforcement and the bonded interface. Appropriate constitutive models were assigned to each component in order to reproduce their respective mechanical behaviour during the debonding process. The masonry substrate was represented by assigning independent material properties to the masonry units and mortar joints, thereby accounting for the heterogeneous nature of masonry. Two masonry configurations were considered in the present study, namely a red brick substrate with cementitious mortar joints and a tuff stone substrate with lime mortar joints.

The FRP reinforcement was modelled as a linear elastic material throughout the analyses. Three FRP systems with different elastic moduli were considered, corresponding to basalt (B-FRP), carbon (C-FRP) and high-modulus carbon (HM-FRP) composites. Owing to the brittle behaviour and high stiffness of the FRP materials, failure of the reinforcement itself was not considered, since all numerical simulations were governed by interfacial debonding prior to reaching the tensile capacity of the FRP.

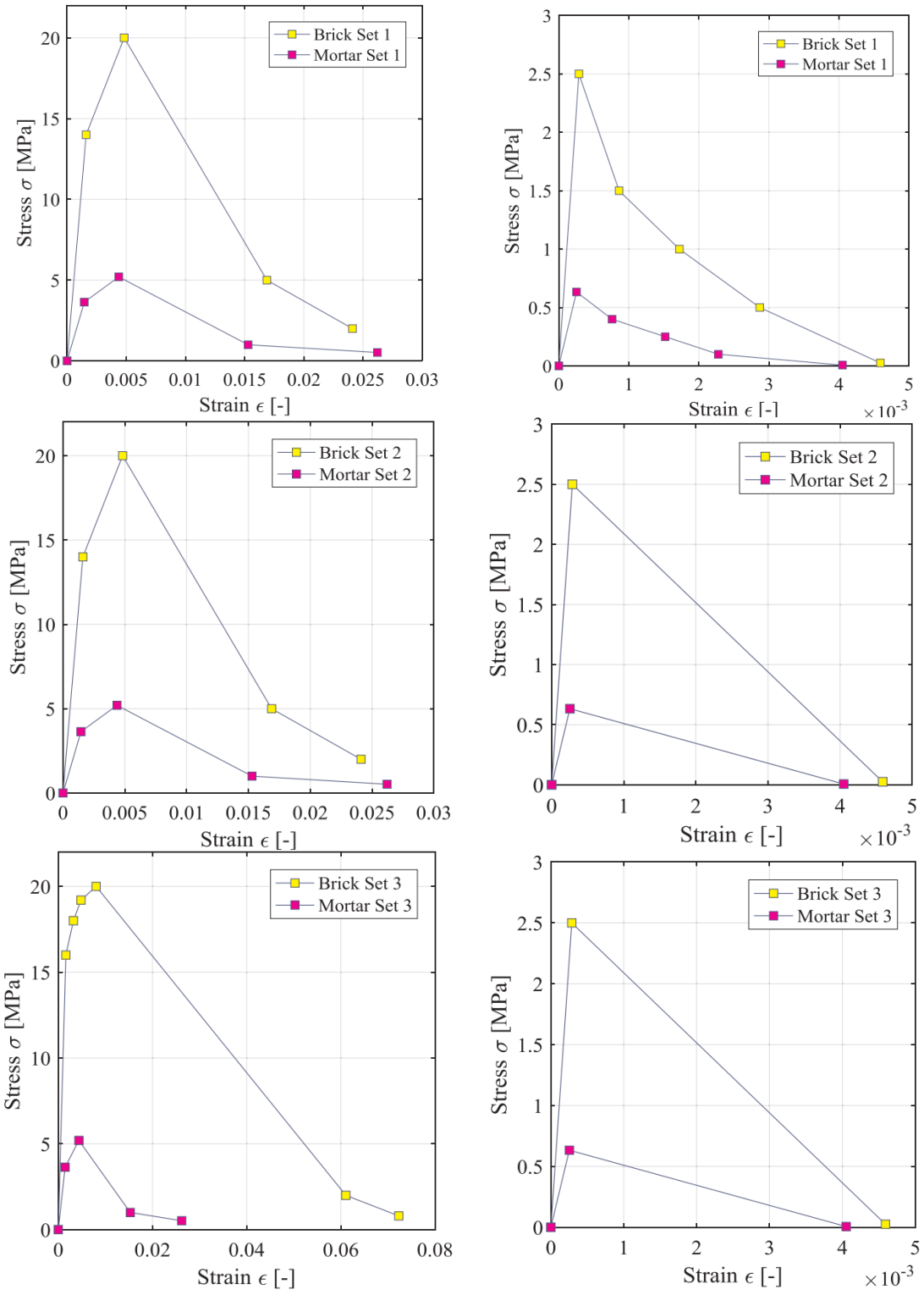
The elastic material properties adopted in the finite element model are summarized in Table 3.2.

Table 3.2: Elastic material properties adopted for the finite element model.

Material	**Young's Modulus, E [MPa]**	**Poisson's Ratio, ν**
Red Brick	8712	0.10
Tuff Stone	3440	0.10
Cementitious mortar	2500	0.10
Lime mortar	2083	0.10
Bassalt (B-FRP)	50000	0.20
Carbon (C-FRP)	240000	0.20
High Mudulus Carbon (HM-FRP)	400000	0.20

The nonlinear behaviour of the masonry materials was represented using the Concrete Damage Plasticity (CDP) model available in Abaqus. This constitutive model was selected because it enables the simulation of nonlinear compressive behaviour, tensile cracking, stiffness degradation and progressive damage of quasi-brittle materials, making it suitable for modelling masonry subjected to interface debonding. Within the CDP formulation, the compressive response is defined through the relationship between compressive stress and inelastic strain, whereas the tensile response is expressed in terms of tensile stress and cracking strain.

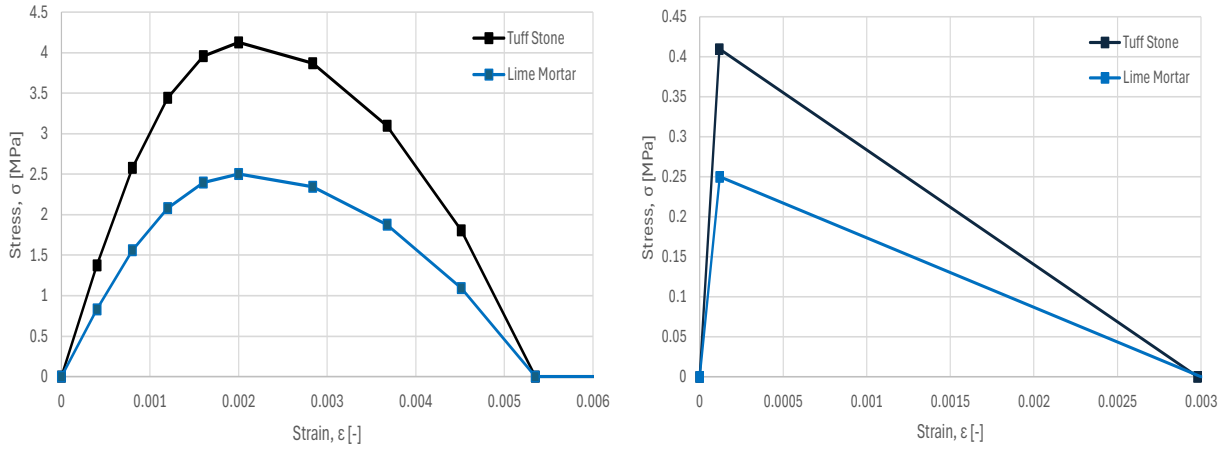
For the brick masonry model, the constitutive relationships of both the clay brick and the cementitious mortar were adopted from the validated numerical study of Bertolesi et al. [27]. As shown in Figure 3.3, Bertolesi et al. proposed three different sets of CDP constitutive relationships (Sets 1–3) for the brick and mortar materials. During the validation stage of the present study, all three material sets were implemented and compared with the available experimental results. Among them, Set 1 provided the closest agreement with the experimental load–displacement response and was therefore adopted for all subsequent numerical analyses and parametric investigations.



(a) uniaxial compression behaviour (b) uniaxial tension behaviour

Figure 3.3 Inelastic mechanical properties adopted for the constituent materials assuming uniaxial compression [27]: (a) uniaxial compressive behaviour; (b) uniaxial tensile behaviour. [27].

For the tuff stone masonry model, the constitutive relationships of the tuff stone and lime mortar were adopted from the experimental and numerical investigations reported by Saviano et al. [39], which provide the mechanical properties representative of traditional Neapolitan tuff masonry. The corresponding compressive and tensile constitutive relationships implemented in the CDP model are presented in Figure 3.4.



(a) uniaxial compression behaviour (b) uniaxial tension behaviour

Figure 3.4: Constitutive relationships adopted for the tuff stone masonry model after Saviano et al. [39]: (a) uniaxial compressive behaviour; (b) uniaxial tensile behaviour.

Since the primary objective of the present study is to investigate the bond behaviour of externally bonded FRP systems, the nonlinear response of the strengthened system was governed by the cohesive interface formulation rather than by failure of the FRP reinforcement itself. Consequently, the FRP reinforcement remained elastic throughout the analyses, while interface damage initiation and propagation were simulated using a cohesive traction–separation formulation. The constitutive model adopted for the cohesive interface is described in the following section.

3.3.3. Interface Modelling and Cohesive Behaviour

The bond between the FRP reinforcement and the masonry substrate was modelled using the surface-based cohesive interaction available in Abaqus/Standard. The cohesive interaction was assigned along the bonded region between the FRP strip and the masonry

substrate in order to simulate the initiation and propagation of interfacial debonding during the loading process. Since interfacial debonding governs the failure of externally bonded FRP systems, the cohesive interface represents the principal nonlinear component of the finite element model.

The interface behaviour was described using a bilinear traction–separation constitutive law. Prior to damage initiation, the interface was assumed to behave linearly elastically and was characterized by independent stiffness coefficients in the normal and tangential directions. After reaching the peak interface strength, progressive stiffness degradation was introduced through a linear energy-based damage evolution law until complete separation of the interface occurred.

The cohesive interface model was first calibrated using the experimental single-lap shear tests on clay brick masonry reported by Bertolesi et al. [27]. Following the validation procedure adopted in the reference study, a single set of cohesive interface properties was assigned along the entire bonded interface, including both the clay brick and the cementitious mortar regions. This modelling strategy was also adopted during the validation stage of the present work to ensure direct comparison with the published numerical results.

The calibrated cohesive properties obtained for the reference FRP–brick interface are summarized in Table 3.3.

Table 3.3: Cohesive interface properties adopted in the finite element model.

Property	Description	Value
K_{nn}	Normal stiffness coefficient (Mode I)	233.7 (MPa/mm)
K_{ss}	Shear stiffness coefficient (Mode II)	106.2 (MPa/mm)
K_{tt}	Secondary shear stiffness coefficient	106.2 (MPa/mm)
t_n^{max}	Maximum nominal normal stress	100 (MPa)
t_n^{max}	Maximum nominal shear stress	2.38 (MPa)
t_n^{max}	Maximum secondary shear stress	2.38 (MPa)
G_f	Fracture energy	0.2383 (N/mm)

For the subsequent parametric analyses, the interface modelling strategy was further extended to account for the heterogeneous nature of masonry. Unlike the validation model, where identical cohesive properties were assigned to both the brick and cementitious

mortar regions, different interface strengths were assigned to the FRP interfaces corresponding to clay brick, tuff stone, cementitious mortar and lime mortar. This modification was introduced to better represent the variation of bond characteristics along the bonded interface when mortar joints are explicitly considered.

The interface strengths were determined according to the CNR-DT 200 recommendation, which relates the peak tangential bond stress to the mechanical properties of the substrate material through

$$f_b = \frac{\sqrt{f_c f_t}}{2} \tag{3.10}$$

where f_c and f_t denote the compressive and tensile strengths of the substrate material, respectively.

The calibrated FRP–brick interface was adopted as the reference case. The interface strengths assigned to the remaining materials were obtained by preserving the proportional relationship predicted by the CNR formulation. Consequently, peak tangential bond strengths of 1.19 MPa, 0.30 MPa, 0.20 MPa and 0.13 MPa were assigned to the FRP–brick, FRP–cementitious mortar, FRP–tuff stone and FRP–lime mortar interfaces, respectively. This approach enables the finite element model to account for the different bond capacities of each substrate material while maintaining consistency with the experimentally calibrated reference interface.

Damage initiation was governed by the Maximum Nominal Stress (MAXS) criterion, whereas the post-peak response was described using a linear energy-based damage evolution law. The fracture energy controls the progressive degradation of the cohesive stiffness and the energy dissipated during crack propagation, allowing the numerical model to reproduce the nonlinear bond–slip response and progressive interface debonding observed experimentally.

The adopted cohesive interface formulation provides a realistic representation of the local stress-transfer mechanism and forms the basis for the subsequent investigation of the influence of FRP stiffness, substrate type and mortar joint discontinuities on the bond behaviour of FRP-strengthened masonry systems.

3.3.4. Boundary Conditions and Loading Procedure

The boundary conditions are defined in a suitable way so as to represent the configuration of the single-lap shear test performed experimentally, while also inhibiting rigid body motion throughout the numerical calculation. From Figure 3.4 it can be seen that the bottom boundary of the masonry substrate is constrained only in the horizontal degrees of freedom (U_1=0), while the upper boundary is constrained only in the vertical degrees of freedom (U_2=0).

A displacement-controlled procedure is used in the analysis to apply the load using a reference point (RP) located on the end of the FRP strip. This reference point is then kinematically tied to the top of the FRP reinforcement in such a way as to transfer displacement evenly to it as the load is increased. Ramp amplitude is used to impose vertical displacement on the reference point using a static general analysis step.

The adopted boundary conditions and loading technique provide a stable and capable representation of progressive debonding and the loading of the specimen as is used experimentally to test the validation cases.

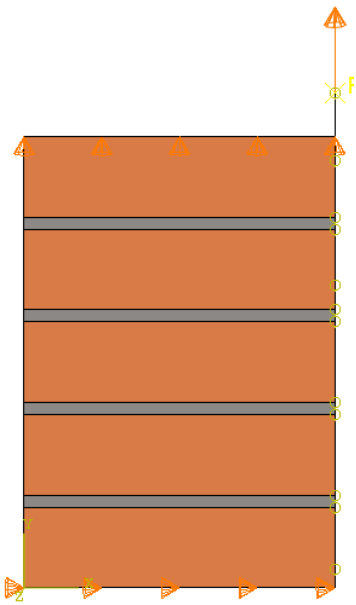


Figure 3.4: Boundary conditions and displacement-controlled loading configuration adopted in the finite element model.

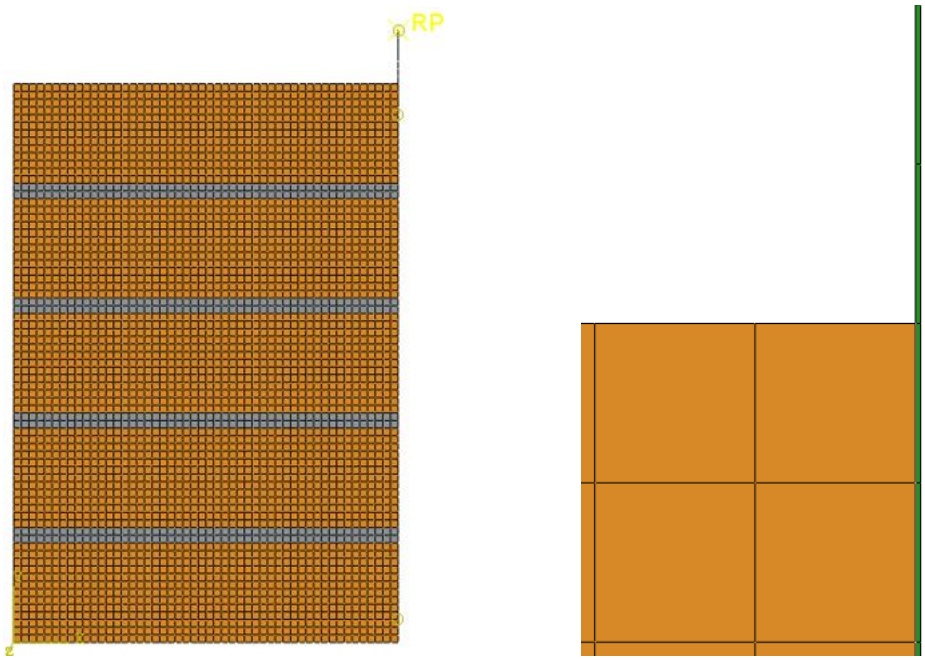
3.3.5. Mesh Discretization and Element Types

In this study, a more sophisticated finite element discretization was used to simulate the transfer of stress and progressive debonding process at the FRP-masonry interface. A 2-D plane strain formulation was used to develop the numerical model which was consistent with the reference numerical study selected for validation.

The brick and mortar regions were meshed separately to model the anisotropic Behaviour of masonry and the discontinuities introduced by mortar joints. Four node bi-linear plane strain quadrilateral elements with reduced integration formulation (CPS4R) were used for masonry and FRP reinforcing layers. Reduced integration formulation was used to enhance computational efficiency while maintaining satisfactory numerical accuracy and convergence stability during the analysis of nonlinearity.

The whole mesh was composed of structured element configuration, which can be observed in Figure 3.5(a). Special meshing refinement was used around mortar joints and the FRP-to-masonry bond interface due to expected stress concentration and localized damage. two elements were used across mortar joint thickness, which is consistent with the reference numerical study to ensure accurate simulation of localized deformation and cracking mechanism in the mortar joint.

The FRP strip was meshed with compatible plane strain quadrilateral elements in the bonded region. Since the thickness of the FRP strip is significantly smaller compared with the dimension of the masonry strip, refined elements in the bond region was chosen and appropriately fitted around the interface to investigate the stress distribution and debonding at the interface between FRP strip and masonry strip. A zoomed view of the bond interface showing the compatible and fitted mesh between the FRP strip and masonry strip is displayed in Figure 3.5(b).



(a) (b)

Figure 3.5: (a) Meshed finite element model; (b) Zoomed view of compatible mesh discretization at the bonded interface.

Surface based cohesive element with a traction-separation law was implemented to simulate the interfacial response between FRP strip and masonry strip. The interface mesh was assumed to be consistent with the adjacent mesh to establish stable stress transfer.

Model Validation

3.4. Model Validation

The finite element model developed in the present study was validated against the numerical investigations reported by Bertolesi et al. [27], who simulated the single-lap shear behaviour of FRP-strengthened brick masonry specimens. The validation aimed to assess the capability of the proposed modelling strategy to reproduce the global bond response and the governing interfacial debonding mechanism before extending the model to the parametric investigations presented in Chapter 4.

The reference study proposed three different sets of masonry constitutive relationships (Sets 1–3) based on the Concrete Damage Plasticity (CDP) model. To ensure a comprehensive validation, the present finite element model was analysed using all three material sets under the same loading configuration adopted in the reference study. The

resulting load–displacement responses were then compared with the published numerical predictions.

Figure 3.6 presents the reference numerical responses reported by Bertolesi et al. [27], while the corresponding responses obtained using the present finite element model are shown in Figure 3.7.

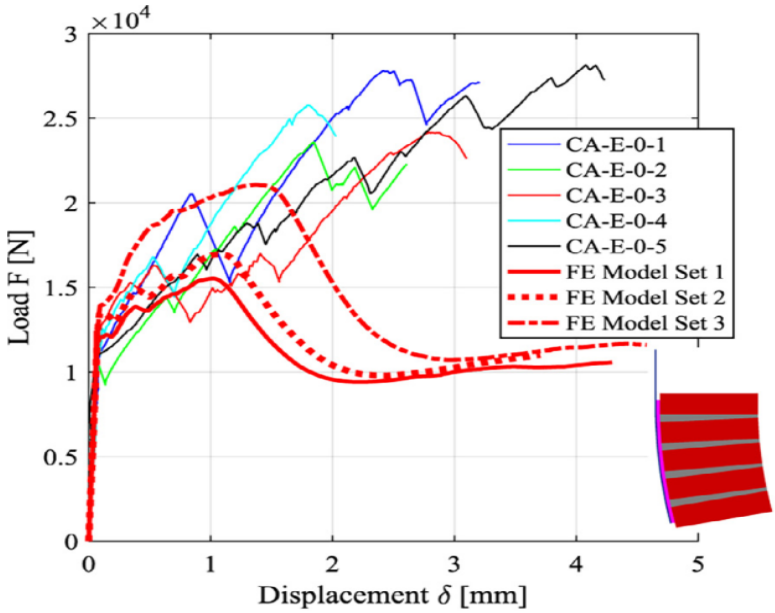


Figure 3.6: Reference numerical load–displacement responses reported by Bertolesi et al. [27]

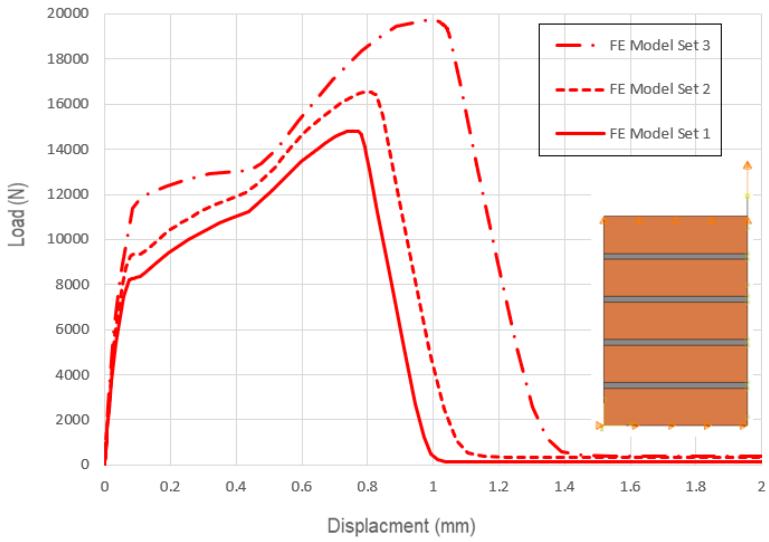


Figure 3.7: Load–displacement responses obtained from the present finite element validation model.

The proposed finite element model successfully reproduces the characteristic response observed in the reference analyses. In all cases, the load initially increases almost linearly as stresses are transferred from the FRP strip to the masonry substrate through the cohesive interface. Following damage initiation, the response becomes nonlinear until the peak bond load is reached, after which progressive interfacial debonding leads to a gradual reduction in the load-carrying capacity.

Although differences in the peak load and post-peak softening are observed, the overall shape of the numerical responses agrees well with the reference results. In particular, the relative behaviour among the three CDP material sets is consistently reproduced, with Set 3 exhibiting the highest bond resistance, followed by Set 2 and Set 1, in agreement with Bertolesi et al. [27]. The remaining discrepancies can be mainly attributed to differences in geometric idealisation, mesh discretisation and numerical implementation of the cohesive interface formulation.

Based on this validation study, the finite element model was considered sufficiently accurate to reproduce the global bond response and the progressive interfacial debonding mechanism of FRP-strengthened masonry systems. Consequently, CDP Material Set 1 was adopted for all subsequent analyses presented in Chapter 4. The selection of Set 1 was motivated by its conservative representation of the masonry behaviour and its suitability for evaluating the influence of substrate type, mortar joint discontinuities and FRP stiffness on the bond behaviour without introducing additional variability associated with different masonry constitutive models.

The validated modelling strategy was subsequently extended beyond the original reference study by incorporating material-dependent cohesive interface properties for the brick, tuff stone, cementitious mortar and lime mortar interfaces, enabling a more realistic representation of heterogeneous masonry systems during the parametric investigation.

4. RESULTS AND DISCUSSIONS

4.1. FRP Strip Bonded to Homogeneous substrate

The first phase of the numerical investigation studies the debonding of externally bonded FRP strips onto a homogeneous substrate without mortar joint discontinuities. In this simulation, the substrate is considered to be one solid block so as to provide a baseline bond response, and the effect of mortar joints can be disregarded in the analysis of the interfacial response.

The homogeneous substrate model represents a relatively simple system to study the impact of both the mechanical Behaviour of the FRP and the substrate material properties on the bond Behaviour. This analysis therefore discusses the impact of those parameters on the load-displacement curve, the ultimate load bearing capacity, the effective bond length and the bond stress distribution across the interface, before additional complications such as masonry with mortar joints are analyzed. The configuration for the homogeneous substrate model is shown in Figure 4.1.

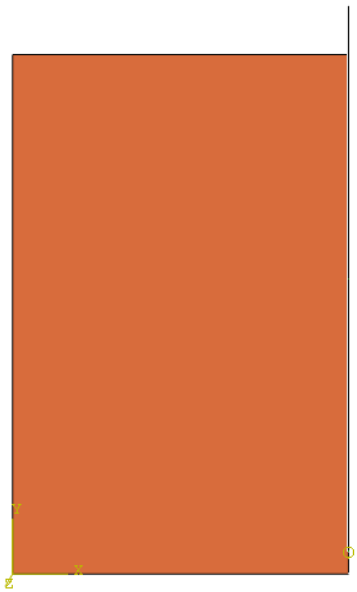


Figure 4.1: Schematic of FRP strip bonded to homogeneous substrate.

4.1.1. Influence of FRP Axial Stiffness and Substrate Properties on Bond Behaviour

Bond performance of the homogeneous specimens was evaluated by investigating the load–displacement response of three FRP systems with different elastic moduli (B-FRP, C-FRP, and HM-FRP) bonded to homogeneous red brick and stone substrates under identical bonding conditions. The objective was to examine the influence of FRP axial stiffness and substrate mechanical properties on the bond behaviour.

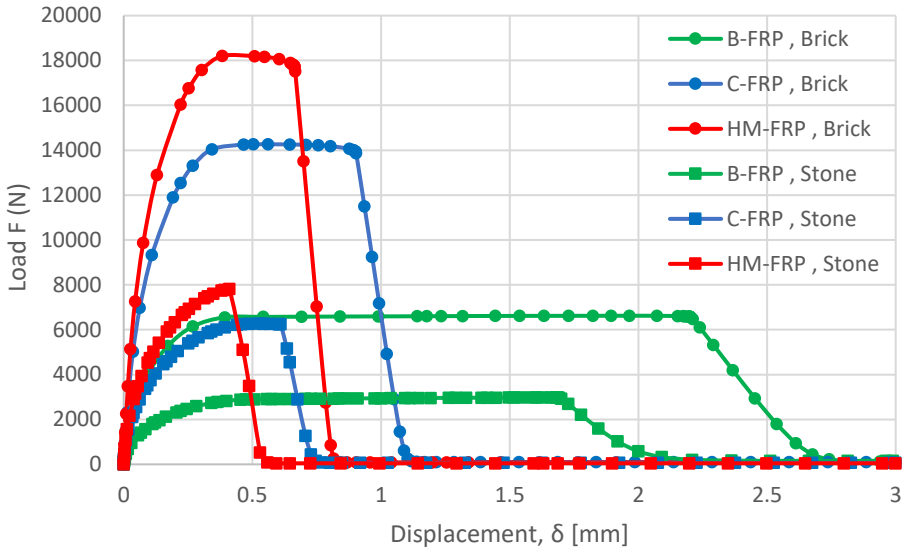


Figure 4.2: Effect of substrate and FRP system on the load–displacement response.

Figure 4.2 shows that increasing the FRP axial stiffness significantly enhances the peak bond load for both substrates. Compared with the B-FRP system, which exhibits the lowest bond capacity and the largest displacement prior to debonding, the HM-FRP system develops the highest peak load but fails after a considerably smaller displacement, indicating a more brittle bond failure. In addition, the red brick substrate consistently develops higher bond loads than the stone substrate for all FRP systems. This Behaviour is attributed to the superior mechanical properties of the red brick, including its higher Young's modulus (8.7 GPa), tensile strength (2.5 MPa), and interface fracture energy (0.2383 N/mm), which allow larger interfacial stresses to develop before debonding.

To further quantify the influence of FRP axial stiffness, the peak bond loads are plotted as a function of the FRP axial stiffness in Figure 4.3.

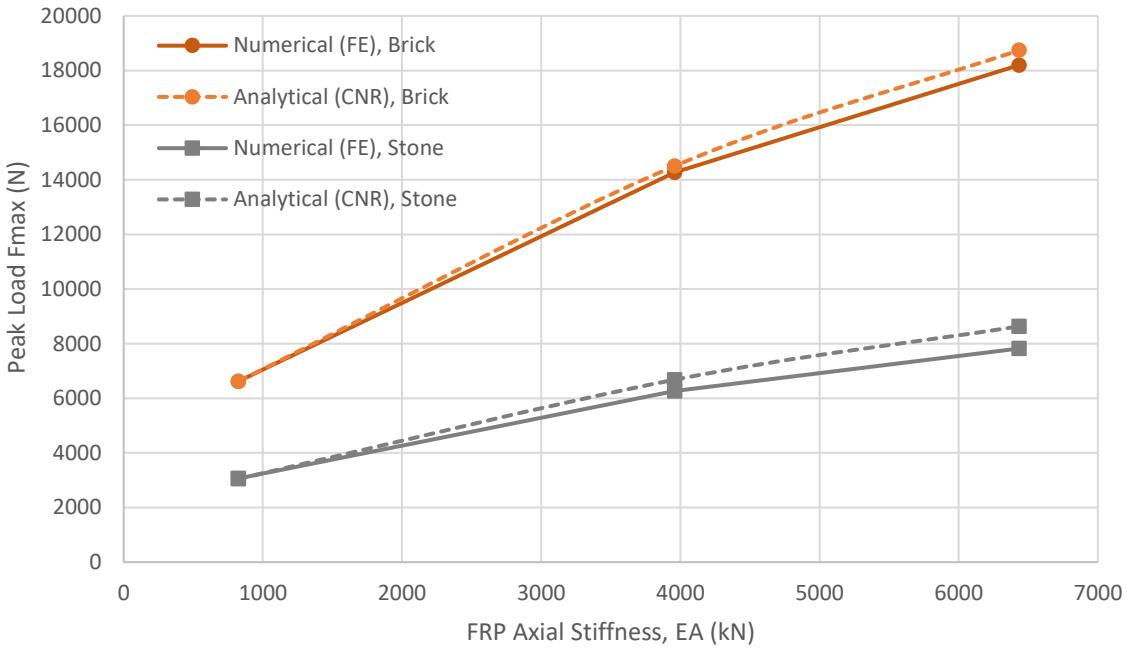


Figure 4.3: Comparison between the FE numerical results and the CNR analytical predictions for the peak bond load as a function of FRP axial stiffness.

Figure 4.3 demonstrates that the peak bond load increases with FRP axial stiffness for both substrates. However, the increase is nonlinear, with progressively smaller gains observed from C-FRP to HM-FRP, indicating diminishing improvements in bond capacity at higher stiffness levels. This trend agrees with the CNR-DT 200 R1 guideline, which relates the maximum transferable bond force to (4.1)

$$\mathrm{F_{max}} \propto \sqrt{\mathrm{E_f\, t_f\, \Gamma_F}} \tag{4.2}$$

Since the FRP thickness and the interfacial properties remained constant for each homogeneous substrate, the relative increase in bond capacity depends primarily on the square root of the FRP elastic modulus. Therefore, the relative bond capacity predicted by the CNR formulation was calculated as:

$$R_{F_{max}}^{CNR} = \frac{F_{max_{e,i}}^{CNR}}{F_{max_{e,B-FRP}}^{CNR}} = \sqrt{\frac{E_{f,i}}{E_{f,B-FRP}}} \tag{4.2}$$

where the B-FRP specimen was adopted as the reference case.

Table 4.1: Comparison between the FE numerical results and the CNR analytical predictions of peak bond load

Substrate	FRP	Bond Length	FE Peak Load	CNR Relative Peak Load	Difference
Brick	B-FRP	330 (mm)	6622.52 (N)	6622.52 (N)	0 (%)
Brick	C-FRP	330 (mm)	14266.20 (N)	14503.32 (N)	-1.6 (%)
Brick	HM-FRP	330 (mm)	18200.60 (N)	18742.73 (N)	-2.9 (%)
Stone	B-FRP	550 (mm)	3065.32 (N)	3065.32 (N)	0 (%)
Stone	C-FRP	550 (mm)	6269.76 (N)	6712.35 (N)	-6.2 (%)
Stone	HM-FRP	550 (mm)	7822.58 (N)	8673.95 (N)	-9.4 (%)

The comparison presented in Table 4.1 demonstrates excellent agreement between the FE numerical results and the CNR analytical predictions for the brick substrate, with differences below 3%. For the stone substrate, the agreement remains satisfactory, although the discrepancies increase to approximately 6–10%. Since all specimens considered in this comparison possess sufficient bond length to fully develop the effective bond length, the remaining differences are more likely associated with the simplified assumptions of the analytical formulation. As the CNR model was originally developed and calibrated for conventional cementitious substrates, the present results suggest that its direct application to natural stone masonry may require substrate-specific calibration to accurately represent the bond behaviour. Nevertheless, the analytical model successfully reproduces the overall increase in bond capacity with increasing FRP axial stiffness.

4.1.2. Interfacial Stress Transfer Mechanism and Effective Bond Length

The load–displacement responses discussed in the previous section provide the global bond Behaviour of the FRP–substrate system; however, they do not reveal how the applied load is transferred through the bonded interface. To investigate the debonding mechanism, the stress field within the substrate and the interfacial shear stress distributions were analyzed throughout the loading process.

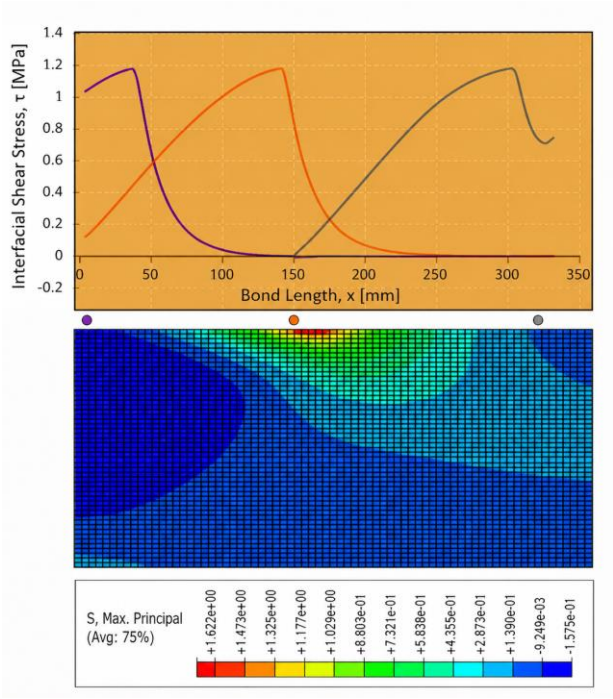


Figure 4.4: Stress redistribution associated with the interfacial shear stress distribution.

Figure 4.4 illustrates the principal stress distribution developed in the substrate immediately prior to interface debonding. The highest stress concentration is observed near the loaded end of the FRP strip, confirming that this region governs the initiation of interface damage. Away from the loaded end, the stress magnitude progressively decreases, indicating that only a limited portion of the bonded interface is effectively mobilized to transfer the applied load. This active stress-transfer region defines the effective bond length, which forms the basis of the bond model adopted in the CNR-DT 200 guideline.

According to the CNR formulation, the transferred bond force is obtained by integrating the interfacial shear stress over the bonded length,

$$F = \int_0^{l_b} \tau(x)\ b_f\, dx \qquad (4.3)$$

where $\tau(x)$ is the interfacial shear stress, b_f is the FRP width, and l_b is the bonded length. Consequently, the effective bond length is defined as the minimum bonded length capable of transferring the maximum bond force. The CNR guideline further relates the effective bond length to the material properties by

$$l_e = \sqrt{\frac{\pi^2 E_f t_f}{2 f_{ctm}}} \qquad (4.4)$$

showing that the effective bond length increases with the FRP axial stiffness and decreases with increasing substrate tensile strength.

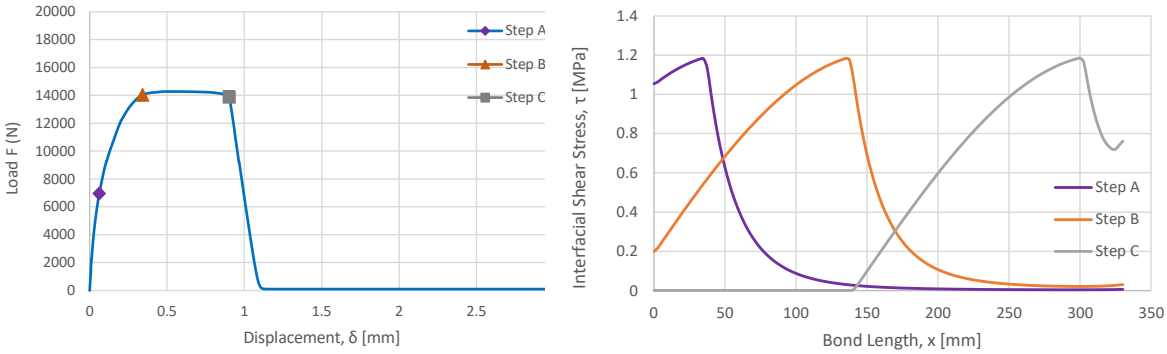


Figure 4.5: Evolution of the interfacial shear stress distribution during debonding.

The evolution of the interfacial shear stress during loading is illustrated in Figure 4.5. At the initial loading stage (Step A), the shear stress is highly concentrated near the loaded end of the bonded interface. As the applied load increases toward the peak load (Step B), the stress-transfer region progressively extends along the bonded length. During the post-peak stage (Step C), interface damage propagates toward the free end, and the active stress-transfer region reaches its maximum extent, corresponding to the effective bond length.

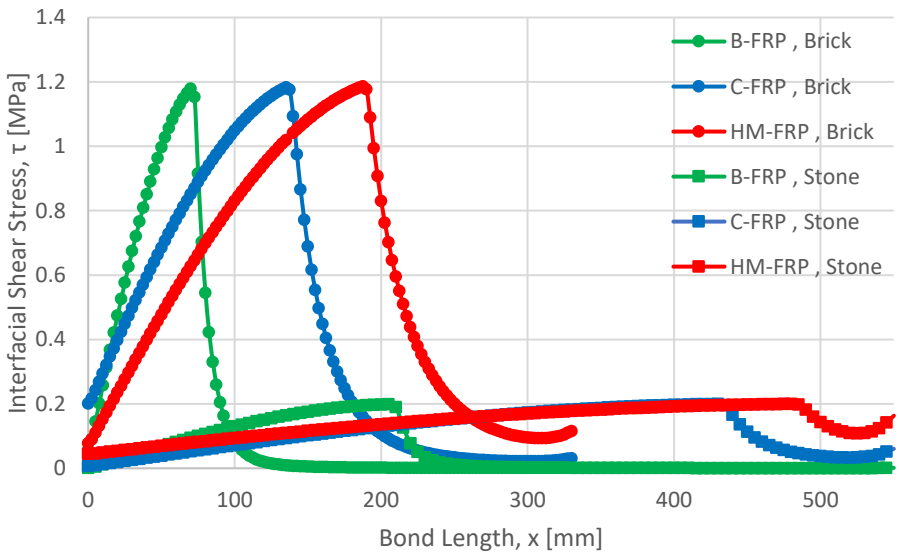


Figure 4.6: Interfacial shear stress distribution for different FRP–substrate combinations.

Figure 4.6 shows that increasing the FRP axial stiffness progressively extends the stress-transfer region for both substrates, resulting in a larger effective bond length. For the red brick substrate, the effective bond length increases from approximately 80 mm for B-FRP to 182 mm for C-FRP and 210 mm for HM-FRP. For the stone substrate, the corresponding values increase from approximately 210 mm to 490 mm and 530 mm, respectively. Owing to its lower stiffness and tensile strength, the stone substrate transfers the applied load over a considerably longer bonded length than the red brick substrate.

To further evaluate the numerical results, the effective bond lengths obtained from the FE simulations were compared with the analytical predictions derived from the CNR formulation. According to Eq. (4.4), the effective bond length is proportional to

$$l_e \propto \sqrt{\frac{E_f t_f}{f_{ctm}}} \tag{4.5}$$

Since the FRP thickness and the substrate tensile strength remained constant within each substrate series, the relative variation of the effective bond length depends only on the FRP elastic modulus. Therefore, the relative effective bond length predicted by the CNR formulation can be expressed as

$$R_{l_e}{}^{CNR} = \frac{{l_{e,i}}^{CNR}}{{l_{e,B-FRP}}^{CNR}} = \sqrt{\frac{E_{f,i}}{E_{f,B-FRP}}} \tag{4.6}$$

where the B-FRP specimen is taken as the reference configuration.

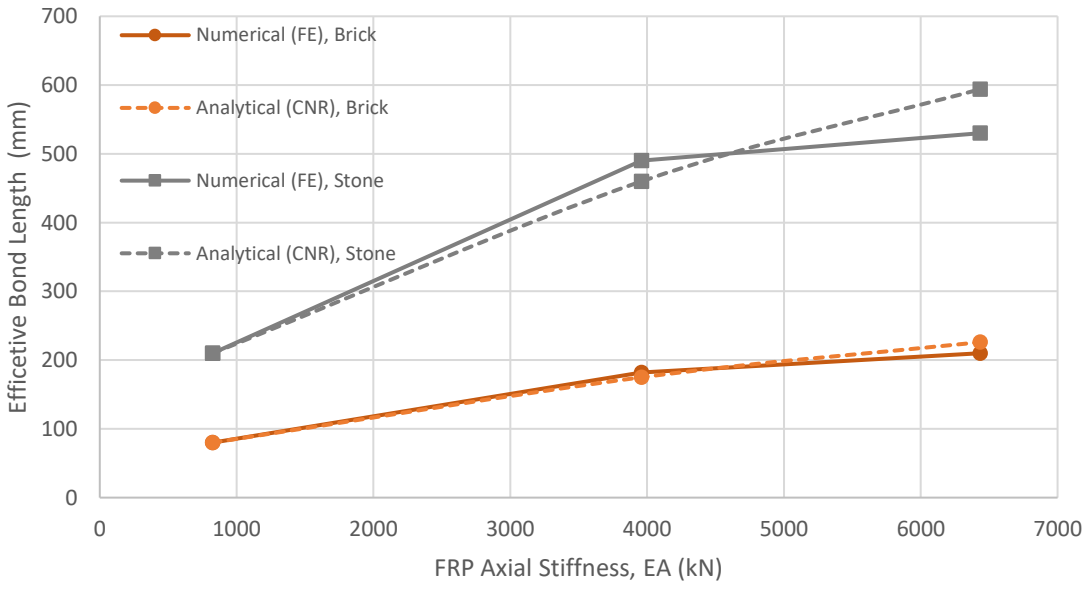


Figure 4.7: Comparison between the effective bond lengths obtained from the finite element (FE) simulations and the corresponding predictions from the CNR analytical formulation for different FRP axial stiffness values.

Table 4.2: Comparison between the FE numerical results and the CNR analytical predictions for the effective bond length of different FRP–substrate combinations.

Substrate	FRP	FE Effective Bond Length	CNR Effective Bond Length	Difference
Brick	B-FRP	80 (mm)	80 (mm)	0 (%)
Brick	C-FRP	182 (mm)	175 (mm)	+4 (%)
Brick	HM-FRP	210 (mm)	226 (mm)	-7.1 (%)
Stone	B-FRP	210 (mm)	210 (mm)	0 (%)
Stone	C-FRP	490 (mm)	460 (mm)	+6.5 (%)
Stone	HM-FRP	530 (mm)	594 (mm)	-10.8 (%)

Figure 4.7 and Table 4.2 compare the effective bond lengths obtained from the FE simulations with the corresponding analytical predictions. Excellent agreement is observed for the brick substrate, with differences below approximately 7%, while the stone substrate exhibits slightly larger deviations of up to approximately 11%. Nevertheless, both the numerical and analytical approaches consistently predict the increase in effective bond length with increasing FRP axial stiffness. The remaining discrepancies can be attributed to the simplifying assumptions inherent in the analytical formulation, whereas the finite element model captures the complete nonlinear stress-transfer process and progressive interface damage. Overall, the CNR formulation provides satisfactory predictions of the effective bond length for both substrate types.

4.2. Influence of Mortar Joints on the FRP–Masonry Bond Mechanism

Unlike the homogeneous substrate investigated in Section 4.1, practical masonry structures contain mortar joints that interrupt the continuity of the bonded interface due to their mechanical properties differing from those of the masonry units. These local variations in stiffness and strength modify the stress-transfer mechanism along the interface. This section investigates the influence of mortar joints on the bond behaviour of externally bonded FRP strips, with particular emphasis on the effects of mortar thickness, FRP axial stiffness, substrate type, and bonded length. The numerical results are interpreted using the concepts of effective bond length and interfacial stress transfer established in the previous section.

4.2.1. Overall Influence of Mortar Joints on Bond Capacity

The introduction of mortar joints modifies the bond behaviour by interrupting the continuity of the bonded interface. To provide an overall assessment of this effect, the peak bond loads obtained for different FRP axial stiffnesses, mortar thicknesses and substrate types are compared.

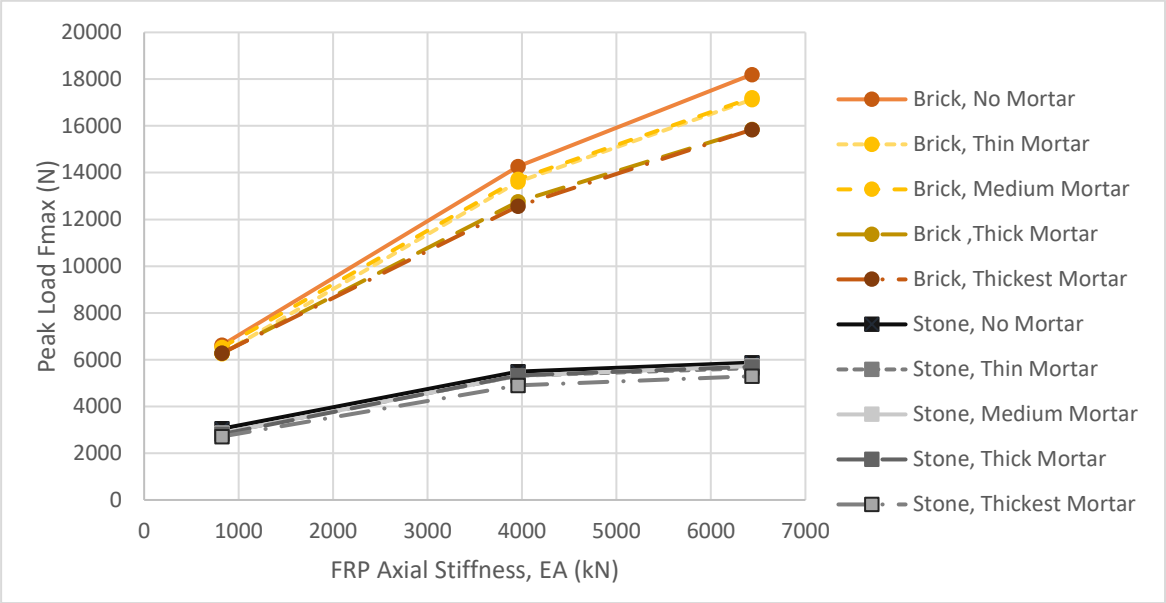


Figure 4.8: Peak load capacity as a function of FRP axial stiffness for different substrates and mortar thicknesses.

Figure 4.8 shows that the peak bond load increases with increasing FRP axial stiffness for both the brick and stone substrates, following the same general trend observed for the homogeneous substrate. However, the presence of mortar joints consistently reduces the bond capacity, and this reduction becomes more pronounced as the mortar thickness increases.

For the brick substrate, the influence of mortar thickness is significant, with the no-mortar configuration providing the highest peak load and progressively thicker mortar joints resulting in lower bond capacities. In contrast, the stone substrate exhibits relatively small differences between the various mortar thicknesses, indicating that the influence of mortar thickness is less pronounced. This difference can be explained by the shorter effective bond length of the stiffer brick substrate. Since the load is transferred over a shorter bonded

region, a larger proportion of the active bond length is occupied by the mortar joint, making the joint thickness more influential. Conversely, the stone substrate develops a much longer effective bond length, allowing the stresses interrupted by the mortar joint to be redistributed over a larger bonded region and reducing the influence of joint thickness.

The global trends presented in Figure 4.8 indicate that the reduction in bond capacity is governed by the combined influence of FRP stiffness, substrate properties and mortar thickness. The mechanisms responsible for these observations are examined in the following sections through the analysis of the load–displacement response and interfacial stress transfer.

4.2.2. Effect of Mortar Joints on the Global Bond Response

Following the overall comparison of peak bond capacities, the influence of mortar joints on the complete load–displacement response is studied. Figure 4.9 compares the responses of the three FRP systems bonded to the brick and stone substrates for the thickest mortar configuration.

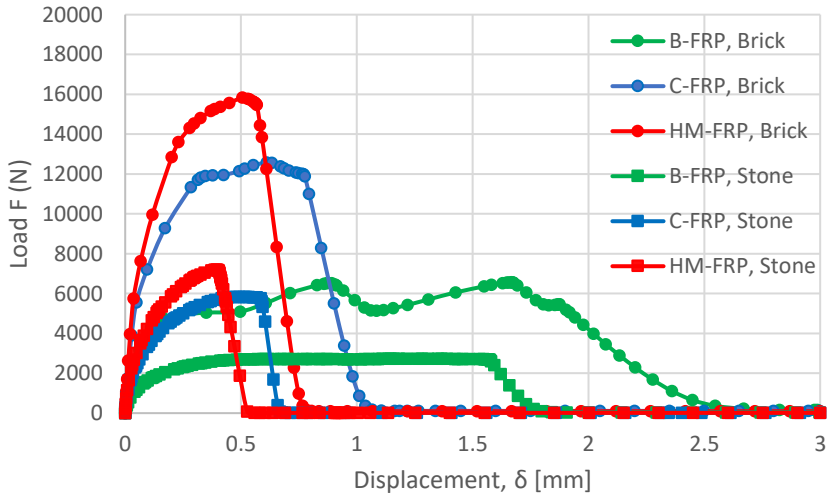


Figure 4.9: Effect of substrate and FRP system on the load–displacement response for the thickest masonry mortar layer.

As shown in Figure 4.9, the general Behaviour remains consistent with that observed for the homogeneous substrate, with the peak bond load increasing from B-FRP to C-FRP and HM-FRP, while the brick substrate develops higher bond capacities than the stone substrate. However, the presence of mortar joints modifies the shape of the response by reducing the length of the plateau and promoting earlier softening after the peak load.

The effect is most evident for the HM-FRP system, where the load drops abruptly after reaching the peak, indicating a more brittle debonding process. In contrast, the B-FRP system retains a more gradual post-peak response and larger displacement capacity, while the C-FRP system exhibits intermediate Behaviour.

These observations indicate that mortar joints influence not only the peak bond load but also the global debonding Behaviour. The mechanisms responsible for these changes are examined in the following section through the analysis of the interfacial shear stress evolution.

4.2.3. Effect of Mortar Joints on the Stress-Transfer Mechanism

Unlike the homogeneous substrate, the masonry model contains multiple interface regions between the FRP strip and the different masonry constituents, including brick, stone, cementitious mortar and lime mortar. Accordingly, different interface properties were assigned to each material based on the calibration procedure described in Section 3.X. The interface bond strengths were determined according to the CNR-DT 200 guideline and calibrated with the reference FRP–brick interface, while the remaining interfaces were defined proportionally according to the mechanical properties of the corresponding substrate materials.

This modelling approach enables the numerical model to capture the variation in interfacial behaviour along the bonded length and to investigate how mortar joints influence the stress-transfer mechanism and the overall bond performance.

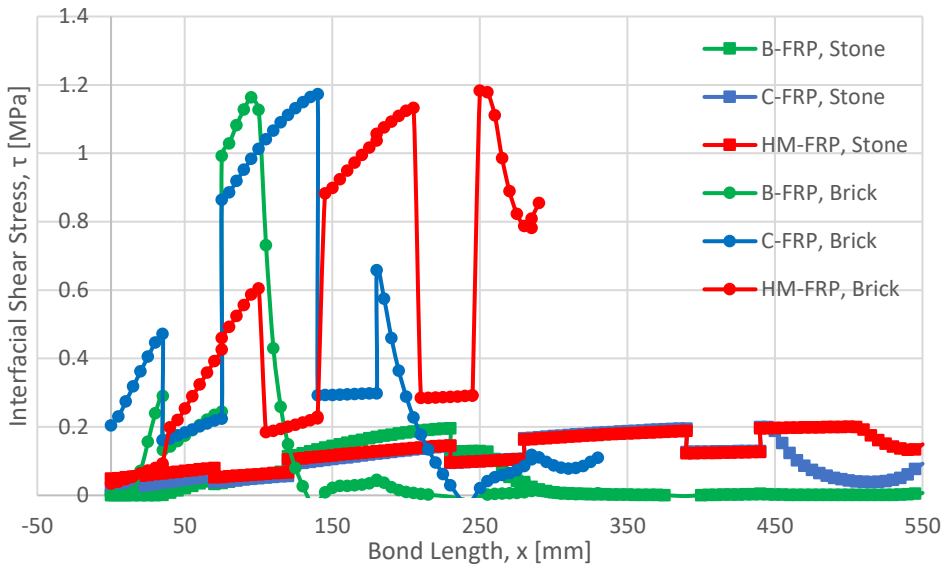


Figure 4.10: Interfacial shear stress distribution for different FRP–substrate combinations at the maximum masonry mortar thickness.

Figure 4.10 shows that, unlike the continuous stress transfer observed for the homogeneous substrate, the interfacial shear stress is interrupted whenever it reaches a mortar joint due to the lower bond strength of the mortar interface and the lower stiffness of the mortar compared with the adjacent masonry units. After crossing the joint, the stress is progressively re-established within the following masonry unit, resulting in a segmented stress-transfer mechanism. This stress redistribution enables the interface to continue transferring the applied load, although with reduced efficiency compared with the homogeneous substrate.

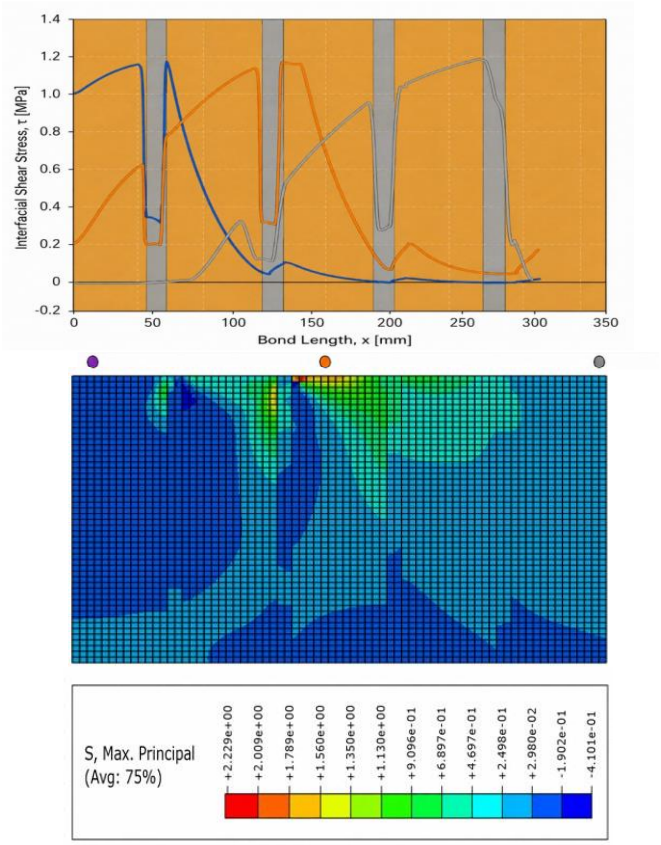


Figure 4.11: Stress redistribution associated with the interfacial shear stress distribution at with mortar effect.

Figure 4.11 provides further insight into the effect of mortar joints on the stress-transfer mechanism. The maximum principal stress contour shows that tensile stresses are primarily concentrated within the masonry units, whereas a noticeable reduction in stress occurs at the mortar joints due to their lower bond strength and stiffness. After crossing each mortar joint, the stresses gradually increase again within the adjacent masonry unit as load transfer continues. This Behaviour is consistent with the periodic reductions observed in the interfacial shear stress distributions, confirming that the presence of mortar joints locally modifies the stress-transfer path and reduces the efficiency of load transfer compared with the homogeneous substrate.

To further illustrate this mechanism, the evolution of the interfacial shear stress is examined at three characteristic stages of the debonding process.

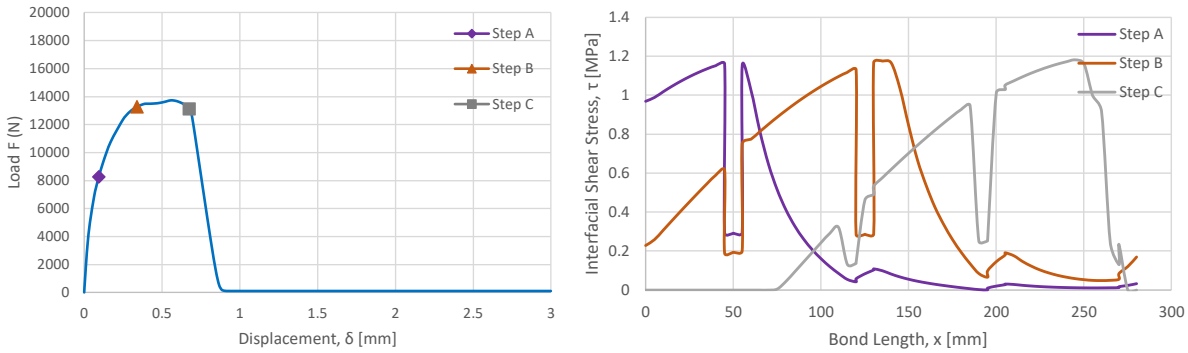


Figure 4.12: Evolution of the interfacial shear stress distribution during debonding at the maximum masonry mortar thickness.

During Step A, the stresses are mainly confined to the first masonry unit. As loading progresses to Step B and Step C, the stresses propagate across successive mortar joints and are repeatedly re-established within the adjacent masonry units. This confirms that, unlike the homogeneous substrate, load transfer occurs through a segmented rather than continuous stress-transfer mechanism.

4.2.4. Effect of Mortar Joints Under Different Bond Length Conditions

The influence of mortar joints on the bond behaviour depends not only on the presence of the mortar layer but also on the relationship between the available bond length and the effective bond length required to fully develop the interfacial stresses. To demonstrate this interaction, three representative specimens with different bonded lengths are selected.

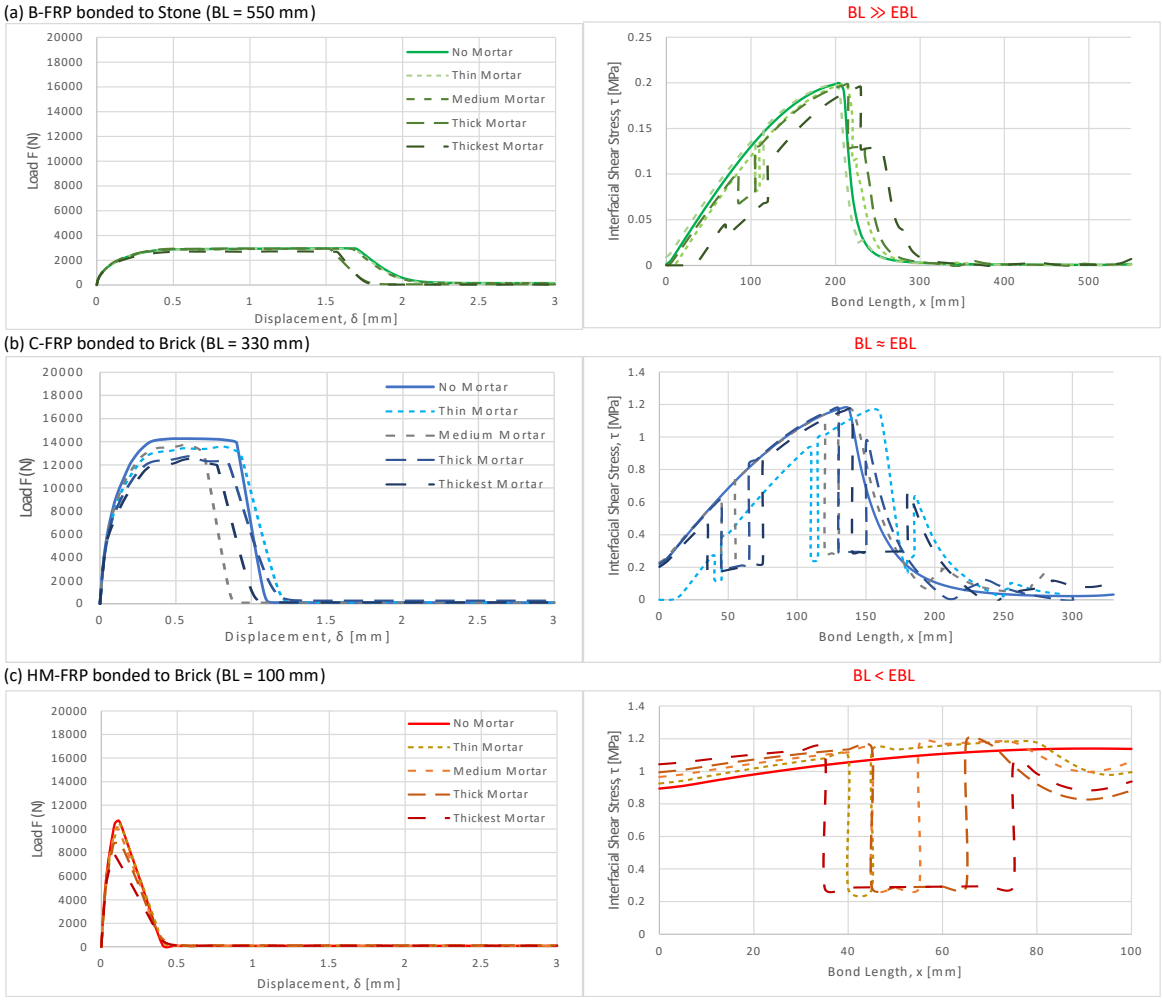


Figure 4.13: Effect of masonry mortar thickness on the load–displacement response and interfacial shear stress distribution for (a) BL > EBL, (b) BL ≈ EBL, and (c) BL < EBL.

For the B-FRP specimen bonded to the stone substrate (Figure 4.13(a)), the available bond length (550 mm) is much greater than the effective bond length. Although the mortar joints locally interrupt the interfacial shear stress, the stresses are recovered in the subsequent masonry units, resulting in only a negligible reduction in the peak bond load.

For the C-FRP specimen bonded to the brick substrate (Figure 4.13(b)), the available bond length (330 mm) is approximately equal to the effective bond length. In this case, the stresses lost within the mortar layer are largely recovered in the adjacent brick unit, allowing most of the bond capacity to be maintained with only a moderate reduction in peak load.

A different response is observed for the HM-FRP specimen bonded to the brick substrate (Figure 4.13(c)), where the available bond length (100 mm) is shorter than the effective bond length. Consequently, the interrupted stresses cannot be fully recovered after crossing

the mortar joint, leading to a premature end of the plateau region and a significant reduction in the peak bond load.

Overall, the results demonstrate that the influence of mortar joints is governed not only by the relationship between the available and effective bond lengths, but also by the local bond strength and the relative stiffness of the substrate components. When sufficient bonded length remains after the mortar joint, the interface can recover the interrupted stress transfer with only a limited loss of bond capacity. Conversely, insufficient bonded length prevents complete stress recovery, resulting in a more pronounced reduction in the transferred load. Furthermore, the local bond strength limits the maximum transferable interfacial stress, while the stiffness mismatch between the mortar joint and the masonry units influences the stress-transfer rate, as reflected by the slope of the interfacial shear stress distribution. The associated increase in effective bond length, resulting from the mobilization of additional bonded regions to compensate for the interrupted stress transfer, is quantified in the following section.

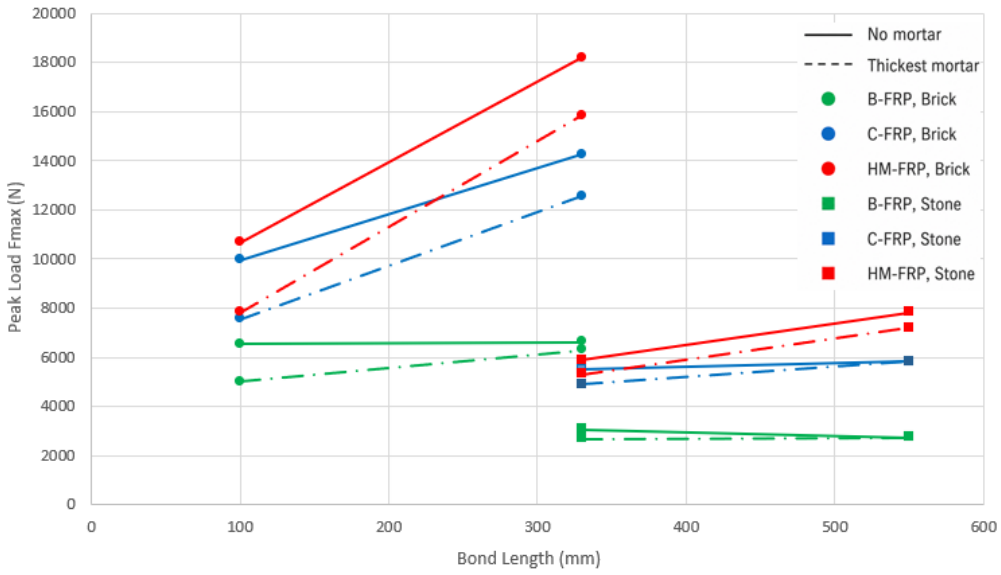


Figure 4.14: Effect of bond length and masonry mortar thickness on peak load capacity.

Figure 4.14 further extends the previous observations by comparing the influence of bond length on the peak bond load for all investigated configurations with and without mortar joints. Nearly horizontal trends indicate that the available bond length is sufficient to fully develop the bond capacity, resulting in only a minor reduction in peak load after introducing

mortar joints. In contrast, the C-FRP and HM-FRP brick specimens exhibit a pronounced increase in peak load with bond length, indicating that the available bonded length is insufficient. Consequently, the interruption of stress transfer at the mortar joints cannot be fully recovered, leading to a more significant reduction in bond capacity. These results confirm that the influence of mortar joints is primarily governed by the relationship between the available and effective bond lengths rather than by the presence of the mortar joints alone.

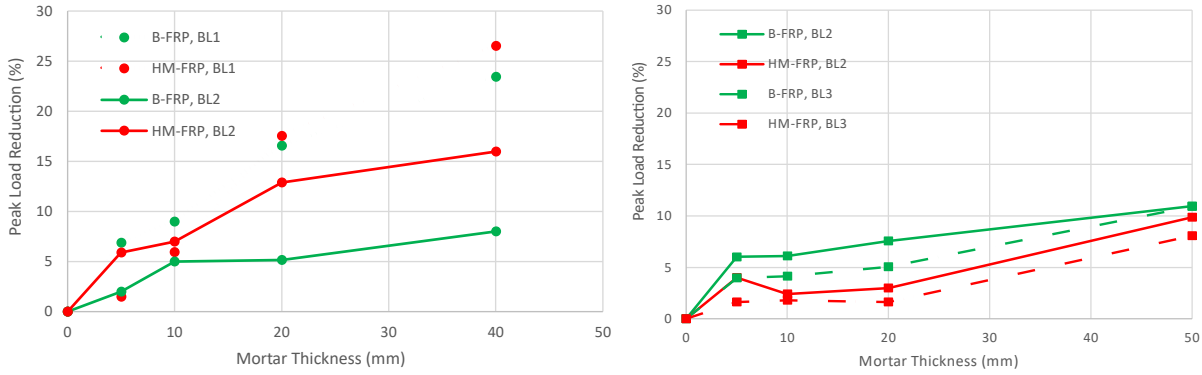


Figure 4.15: Effect of masonry mortar thickness on peak load reduction for different bond lengths.

To quantify the influence of mortar joints, Figure 4.15 presents the percentage reduction in peak bond load with increasing mortar thickness. For the brick substrate, the reduction increases progressively with mortar thickness and is strongly dependent on the available bond length. This greater sensitivity is attributed to the shorter effective bond length of the stiffer brick substrate, where the mortar joint occupies a larger proportion of the active stress-transfer region. Consequently, a greater part of the available bond capacity is affected by the joint, resulting in a larger reduction in peak load. In contrast, the stone substrate develops a considerably longer effective bond length, allowing the interrupted stresses to be redistributed over a larger bonded region. As a result, the peak load reduction remains below approximately 11% even for the thickest mortar joint.

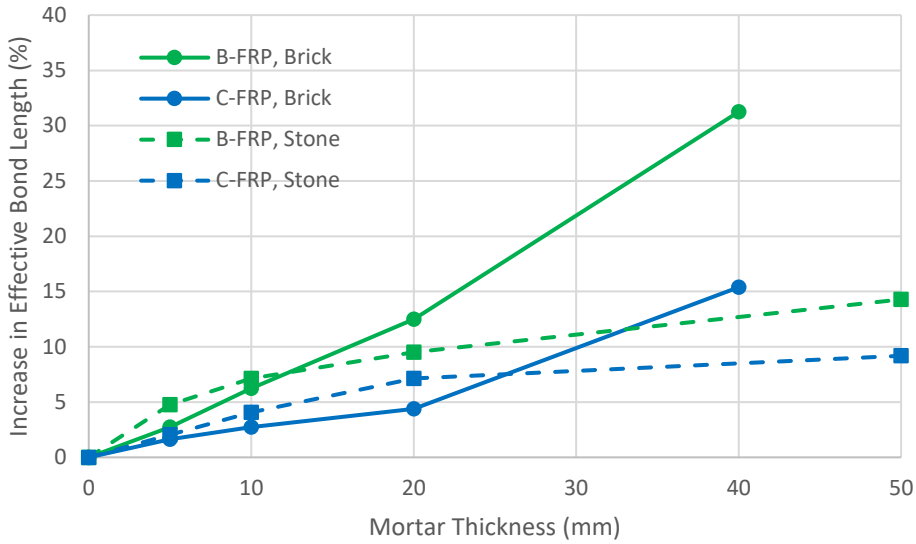


Figure 4.16: Effect of masonry mortar thickness on the effective bond length.

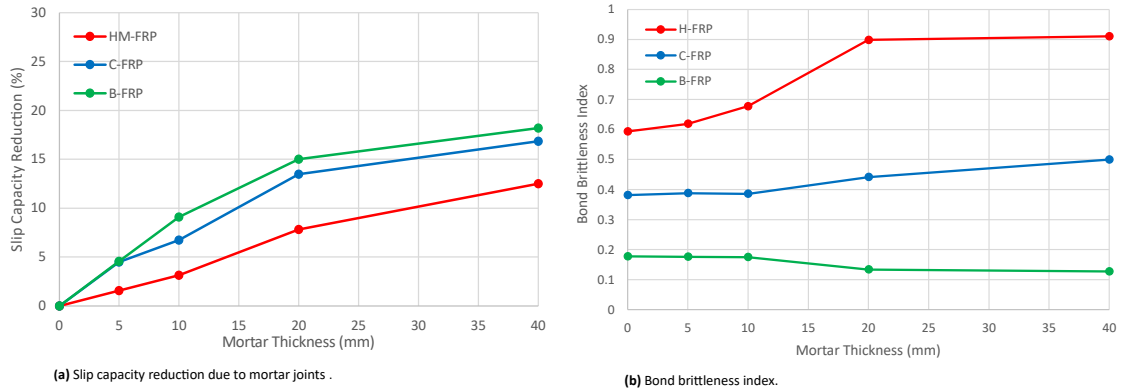
Figure 4.16 further illustrates the increase in effective bond length with increasing mortar thickness. As the mortar joints interrupt the interfacial stress transfer, additional bonded regions are progressively mobilized to recover the lost stresses. Consequently, the effective bond length increases with mortar thickness for both substrates, although the increase is considerably greater for the brick specimens. This behaviour is attributed to the shorter effective bond length of the stiffer brick substrate, where the mortar joint occupies a larger proportion of the active stress-transfer region. As a result, a greater extension of the effective bond length is required to compensate for the interrupted stresses. This increase explains why the reduction in peak bond load remains limited when sufficient bonded length is available, whereas specimens with insufficient bonded length are unable to fully compensate for the stress loss induced by the mortar joints.

4.2.5. Influence of FRP Axial Stiffness and Mortar Joints on Bond Failure Brittleness

In addition to the peak bond load, the deformation characteristics of the bonded interface provide important insight into the bond failure mechanism. While the maximum interface slip represents the overall deformation capacity prior to complete debonding, the post-peak deformation capacity governs the brittleness of the failure process. To quantify this behaviour, a Bond Brittleness Index (I_b) is introduced, defined as the ratio between the interface slip at the peak bond load and the interface slip at complete debonding:

$$I_b = \frac{\delta_{peak}}{\delta_{failure}} \quad (4.7)$$

where δp is the interface slip at the peak bond load and δf is the interface slip at complete debonding. A higher value of Ib indicates that failure occurs shortly after reaching the peak load, corresponding to a more brittle bond response, whereas lower values indicate greater post-peak deformation capacity and a more progressive debonding process.



(a) Slip capacity reduction due to mortar joints .

(b) Bond brittleness index.

Figure 4.17: Influence of masonry mortar thickness on the bond failure characteristics: (a) reduction in interface slip capacity; (b) bond brittleness index.

Figure 4.17(a) shows that increasing the mortar thickness progressively reduces the interface slip capacity for all FRP systems, although the magnitude of this reduction depends on the FRP stiffness. The largest reduction is observed for the B-FRP specimens, reaching approximately 18% for the thickest mortar joint, whereas the HM-FRP specimens exhibit a smaller reduction of approximately 13% owing to their inherently lower deformation capacity.

Figure 4.17(b) further demonstrates that the influence of mortar joints on failure brittleness strongly depends on the FRP axial stiffness. The Bond Brittleness Index increases noticeably with increasing mortar thickness for the HM-FRP and C-FRP systems, indicating that the post-peak deformation capacity becomes progressively smaller and the bond failure becomes increasingly brittle. Relative to the no-mortar configuration, the brittleness index increases by approximately 50% for HM-FRP and 31% for C-FRP at the thickest mortar thickness. In contrast, the B-FRP system exhibits a slight reduction in the brittleness index despite the decrease in slip capacity, indicating that its relatively compliant behaviour continues to promote a progressive debonding process even in the presence of mortar joints.

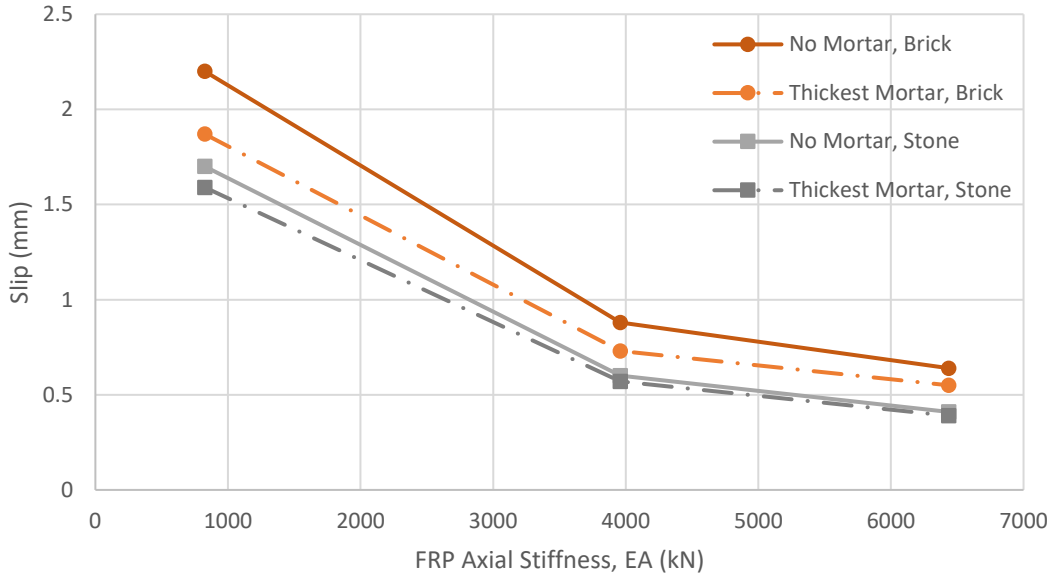


Figure 4.18: Effect of FRP axial stiffness and masonry mortar thickness on slip Capacity (at Failure).

The influence of mortar joints is further quantified in Figure 4.18, which presents the reduction in slip capacity with increasing mortar thickness. For all FRP systems, thicker mortar joints lead to a progressive decrease in the slip prior to debonding, confirming that mortar joints promote a more brittle bond failure. The largest reduction is observed for the B-FRP specimens, while the HM-FRP specimens are less affected due to their inherently smaller deformation capacity.

Finally, it should be noted that none of the investigated configurations reached the tensile capacity of the FRP reinforcement. The theoretical tensile capacities of the B-FRP, C-FRP, and HM-FRP systems (approximately 33 kN, 66 kN, and 66 kN, respectively) were not attained, as interfacial debonding consistently occurred first. This confirms that the bond interface governs the failure of the strengthened system, emphasizing that improving the interfacial bond performance is more critical than simply increasing the tensile capacity of the FRP reinforcement

5. CONCLUSIONS AND FURTHER DEVELOPMENTS

5.1. Conclusions

The present study investigated the bond Behaviour of externally bonded FRP strengthening systems applied to masonry, with particular emphasis on the influence of mortar joints on the interfacial stress-transfer mechanism. A calibrated finite element model was developed and employed to investigate the effects of FRP axial stiffness, substrate type, mortar thickness and bond length on the global bond response, effective bond length and failure mechanism. The numerical investigation also enabled detailed observation of the interfacial stress evolution during debonding, providing insight into mechanisms that are difficult to capture experimentally.

The principal findings of this research are summarized as follows.

- **Influence of FRP stiffness and substrate properties**

Increasing the FRP axial stiffness enhanced the peak bond load for both brick and stone substrates. However, the improvement gradually diminished at higher stiffness levels, indicating diminishing returns with increasing FRP stiffness. The substrate mechanical properties were also found to strongly influence the bond Behaviour. Owing to its higher stiffness and tensile strength, the brick substrate consistently developed higher bond capacities and shorter effective bond lengths than the stone substrate, whereas the weaker stone substrate transferred the applied load over a considerably longer bonded region.
The FE predictions showed excellent agreement with the CNR-DT 200 analytical formulation for brick masonry for both peak bond load and effective bond length. Although the analytical model also captured the overall Behaviour of natural stone masonry, larger deviations were observed, suggesting that substrate-specific calibration may improve the applicability of the CNR formulation to stone substrates.

- **Stress-transfer mechanism and the governing role of effective bond length**

Unlike homogeneous substrates, masonry containing mortar joints exhibited a segmented stress-transfer mechanism in which the interfacial shear stress was locally interrupted at each mortar joint before being progressively re-established within the adjacent masonry unit. This stress recovery mechanism explains why mortar joints do not necessarily produce significant reductions in bond capacity.

The numerical results demonstrated that the influence of mortar joints is governed primarily by the relationship between the available bond length and the effective bond length rather than by the presence of the mortar joints alone. When sufficient bonded length remained available after crossing the mortar joint, the interrupted stresses were almost completely recovered, resulting in only minor reductions in peak bond load. Conversely, insufficient bonded length prevented complete stress recovery, leading to substantial reductions in bond capacity.

Increasing mortar thickness progressively increased the effective bond length by mobilizing additional bonded regions to compensate for the interrupted stress transfer. This effect was considerably greater for the brick substrate because its shorter effective bond length caused the mortar joint to occupy a larger proportion of the active stress-transfer region, making the bond Behaviour more sensitive to mortar thickness than in the stone substrate.

- **Bond failure Behaviour**

The deformation Behaviour demonstrated that increasing the FRP axial stiffness reduced the interface slip prior to failure and promoted progressively more brittle bond Behaviour. To quantify this response, a Bond Brittleness Index was proposed based on the ratio between the interface slip at the peak bond load and the slip at complete debonding. The proposed index showed that increasing mortar thickness significantly increased the brittleness of the HM-FRP and C-FRP systems, whereas the more compliant B-FRP system maintained a relatively progressive post-peak debonding response despite reductions in its overall slip capacity.

Furthermore, none of the investigated configurations reached the tensile capacity of the FRP reinforcement. Interfacial debonding consistently occurred before rupture of the FRP strip, confirming that the bond interface governs the ultimate Behaviour of externally bonded FRP strengthening systems. Consequently, improving the interfacial bond Behaviour is considerably more beneficial than simply increasing the tensile strength of the FRP reinforcement.

- **Overall engineering significance**

The present study demonstrates that the influence of mortar joints cannot be evaluated solely based on their thickness or even their presence. Instead, their effect is controlled by the interaction between substrate mechanical properties, FRP axial stiffness, effective bond length and available bonded length, which together determine the ability of the interface to recover the interrupted stress transfer. These findings provide a more rational understanding of FRP–masonry bond Behaviour and contribute to improving both numerical modelling approaches and analytical design methods for strengthened masonry structures.

5.2. Original Contributions of the Present Study

The principal scientific contributions of this research can be summarized as follows:

- A calibrated finite element model was developed to investigate the bond Behaviour of externally bonded FRP systems applied to masonry containing mortar joints.
- The stress-transfer mechanism of FRP-strengthened masonry was explained through the identification of a segmented stress-transfer process, in which interfacial stresses are interrupted at mortar joints and progressively recovered within adjacent masonry units.
- The study demonstrated that the influence of mortar joints is governed primarily by the relationship between the available bond length and the effective bond length,

providing a physical explanation for the different sensitivity of brick and stone masonry to mortar thickness.

- The increase in effective bond length caused by mortar joints was explained as a stress-compensation mechanism, whereby additional bonded regions are mobilized to recover the stresses interrupted by the mortar joints.
- A comprehensive comparison between FE simulations and the CNR-DT 200 analytical formulation was performed for both peak bond load and effective bond length. While excellent agreement was obtained for brick masonry, the observed deviations for natural stone masonry highlight the need for substrate-specific calibration of existing analytical bond models.
- A Bond Brittleness Index was proposed to quantify the post-peak deformation Behaviour of FRP–masonry interfaces, providing a practical indicator for comparing the brittleness of different FRP strengthening systems.

5.3. Further Developments

The numerical framework developed in this study provides a basis for several future research directions.

First, the proposed stress-transfer mechanism should be validated through dedicated experimental investigations on masonry specimens containing different mortar thicknesses and mortar types. Particular attention should be given to validating the stress recovery process predicted between adjacent masonry units.

Second, the discrepancies observed between the FE simulations and the CNR analytical formulation for natural stone masonry suggest that improved analytical models or substrate-dependent calibration factors should be developed to extend current design recommendations beyond conventional brick masonry.

Future studies should also investigate the influence of additional parameters not considered in the present work, including mortar mechanical properties, adhesive thickness, FRP thickness, FRP width, adhesive properties and interface fracture energy. Such investigations

would provide a more comprehensive understanding of the parameters governing FRP–masonry bond Behaviour.

The developed numerical methodology may also be extended to evaluate the influence of cyclic loading, fatigue, seismic actions and long-term environmental effects such as temperature variation, moisture exposure and ageing, thereby providing a more realistic assessment of the long-term performance of strengthened masonry structures.

Finally, the Bond Brittleness Index proposed in this study should be further validated experimentally and numerically for different strengthening systems, substrate materials and loading conditions. Such investigations may establish the proposed index as a generalized indicator for assessing the post-peak bond failure Behaviour of FRP-strengthened masonry.

THIS PAGE WAS INTENTIONALLY LEFT BLANK

REFERENCES

[1] S. A. Babatunde, “Review of strengthening techniques for masonry using fiber reinforced polymers,” Composite Structures, vol. 161, pp. 246–255, 2017.

[2] H. Ehsani, M. R. Saadatmanesh, and J. L. Velazquez-Dimas, “Behaviour of retrofitted URM walls under simulated earthquake loading,” Journal of Composites for Construction, vol. 3, no. 3, pp. 134–142, 1999.

[3] T. C. Triantafillou, “Strengthening of masonry structures using epoxy-bonded FRP laminates,” Journal of Composites for Construction, vol. 2, no. 2, pp. 96–104, 1998.

[4] S. W. Chuang, Y. Zhuge, Y. Y. Wong, and L. Peters, “Seismic retrofitting of unreinforced masonry walls by FRP strips,” New Zealand Society for Earthquake Engineering Conference Proceedings, pp. 1–8, 2003.

[5] G. Tumialan and A. Nanni, “Strengthening of masonry walls with FRP bars,” Composites Fabrication Magazine, pp. 1–9, 2002.

[6] K. Roko, T. E. Boothby, and C. E. Bakis, “Failure mode of sheet bonded fiber reinforced polymer applied to brick masonry,” in Proc. 4th Int. Symp. Fiber Reinforced Polymer Reinforcement for Reinforced Concrete Structures (FRPRCS-4), Baltimore, MD, USA, 1999, pp. 305–311.

[7] C. Maruccio, I. Basilio, D. V. Oliveira, P. B. Lourenço, and G. Monti, “Numerical modelling and parametric analysis of bond strength of masonry members retrofitted with FRP,” Construction and Building Materials, vol. 73, pp. 713–727, 2014.

[8] H. Hernoune, B. Benabed, R. Abousnina, A. Alajmi, A. M. G. Alfadhili, and A. Shalwan, “Experimental Research and Numerical Analysis of CFRP Retrofitted Masonry Triplets under Shear Loading,” Polymers, vol. 14, no. 18, p. 3707, 2022.

[9] F. Freddi and E. Sacco, “Mortar joints influence in debonding of masonry element strengthened with FRP,” Key Engineering Materials, vol. 624, pp. 197–204, 2015.

[10] B. Ghiassi, D. V. Oliveira, P. B. Lourenço, and G. Marcari, “Numerical study of the role of mortar joints in the bond Behaviour of FRP-strengthened masonry,” Composites Part B: Engineering, vol. 46, pp. 21–30, 2013.

[11] R. Fedele and G. Milani, “Assessment of bonding stresses between FRP sheets and masonry pillars during delamination tests,” Composites Part B: Engineering, vol. 43, no. 4, pp. 1999–2011, 2012.

[12] E. Sassoni, V. Sarti, A. Bellini, C. Mazzotti, and E. Franzoni, “The role of mortar joints in FRP debonding from masonry,” Composites Part B: Engineering, vol. 135, pp. 166–174, 2018.

[13] S. A. Babatunde, “Review of strengthening techniques for masonry using fiber reinforced polymers,” Composite Structures, vol. 161, pp. 246–255, 2017.

[14] S. Xia and D. Oehlers, “Debonding Mechanisms in FRP Plated Unreinforced Masonry Under Out-of-Plane Loading,” Advances in Structural Engineering, vol. 9, no. 5, pp. 619–632, 2006.

[15] T. C. Triantafillou, “Strengthening of masonry structures using epoxy-bonded FRP laminates,” Journal of Composites for Construction, vol. 2, no. 2, pp. 96–104, 1998.

[16] R. B. Petersen, M. J. Masia, and R. Seracino, “Bond Behaviour of Near-Surface Mounted FRP Strips Bonded to Modern Clay Brick Masonry Prisms: Influence of Strip Orientation and Compression Perpendicular to the Strip,” Journal of Composites for Construction, vol. 13, no. 3, pp. 169–178, 2009.

[17] R. B. Petersen, M. J. Masia, and R. Seracino, “In-Plane Shear Behaviour of Masonry Panels Strengthened with NSM CFRP Strips. II: Finite-Element Model,” Journal of Composites for Construction, vol. 14, no. 6, pp. 764–774, 2010.

[18] J. G. Tumialan, N. Galati, S. M. Namboorimadathil, and A. Nanni, “Strengthening of Masonry with FRP Bars,” in ICCI 2002, San Francisco, CA, USA, June 10–12, 2002.

[19] F. Freddi and E. Sacco, “An interphase model for the analysis of the masonry-FRP bond,” Composite Structures, vol. 138, pp. 322–334, 2016.

[20] R. Fedele and G. Milani, “Three-dimensional effects induced by FRP-from-masonry delamination,” Composite Structures, vol. 158, pp. 839–855, 2016.

[21] E. Grande, M. Imbimbo, and E. Sacco, “Bond behaviour of CFRP laminates glued on clay bricks: Experimental and numerical study,” Journal of Composites for Construction, vol. 15, no. 3, pp. 330–340, 2011.

[22] E. Grande and G. Milani, “Modeling of FRP-strengthened curved masonry specimens and proposal of a simple design formula,” Composite Structures, vol. 158, pp. 281–290, 2016.

[23] E. Grande, M. Imbimbo, and E. Sacco, “Simple model for the bond Behaviour of masonry elements strengthened with FRP,” Journal of Composites for Construction, vol. 15, no. 3, pp. 354–363, 2011.

[24] O. Rabinovitch, “An extended high order cohesive interface approach to the debonding analysis of FRP strengthened beams,” International Journal of Mechanical Sciences, vol. 81, pp. 1–16, 2014.

[25] J. G. Teng, H. Yuan, and J. F. Chen, “FRP-to-concrete interfaces between two adjacent cracks: theoretical model for debonding failure,” International Journal of Solids and Structures, vol. 43, no. 18–19, pp. 5750–5778, 2006.

[26] E. Bertolesi, G. Milani, M. Fagone, T. Rotunno, and E. Grande, “Micro-mechanical FE numerical model for masonry curved pillars reinforced with FRP strips subjected to single lap shear tests,” Composite Structures, vol. 201, pp. 916–931, 2018.

[27] T. Rotunno, M. Fagone, E. Bertolesi, E. Grande, and G. Milani, “Single lap shear tests of masonry curved pillars externally strengthened by CFRP strips,” Composite Structures, vol. 200, pp. 434–448, 2018.

[28] CNR-DT 200 R1/2013, “Guide for the Design and Construction of Externally Bonded FRP Systems for Strengthening Existing Structures,” National Research Council of Italy (CNR), Rome, Italy, 2013.

[29] G. Marcari, B. Ghiassi, D. V. Oliveira, and P. B. Lourenço, “Numerical analysis of bond Behaviour between masonry bricks and composite materials,” Engineering Structures, vol. 43, pp. 210–220, 2012.

[30] R. Luccioni and V. C. Rougier, “Shear behaviour of brick–mortar interface in CFRP retrofitted or repaired masonry,” International Journal of Mechanical Sciences, vol. 52, no. 4, pp. 602–611, 2010.

[31] E. Grande, M. Imbimbo, and E. Sacco, “Numerical modelling of FRP-to-masonry debonding behaviour,” Composite Structures, vol. 92, pp. 110–122, 2010.

[32] B. Ghiassi, D. V. Oliveira, and P. B. Lourenço, “A review of bond behaviour between FRP composites and masonry substrates,” Construction and Building Materials, vol. 95, pp. 337–352, 2015.

[33] Abaqus, “Abaqus Analysis User’s Manual, Version 6.14,” Dassault Systèmes Simulia Corp., Providence, RI, USA, 2014.

[34] E. Grande, M. Imbimbo, and E. Sacco, “Modeling of FRP-to-masonry interfaces under mixed-mode loading conditions,” Composite Structures, vol. 94, no. 6, pp. 1848–1859, 2012.

[35] E. Grande, M. Imbimbo, and E. Sacco, “Analytical and numerical study of debonding phenomena in FRP-strengthened masonry structures,” Engineering Fracture Mechanics, vol. 102, pp. 1–18, 2013.

[36] E. Grande, G. Milani, and T. Rotunno, “Modeling of shear-lap tests of flat and curved masonry specimens strengthened by FRCM,” Structures, vol. 52, pp. 437–448, 2023.

[37] R. Dimitri, E. Lucantonio, and F. Tornabene, “Numerical Modeling of Single-Lap Shear Bond Tests for Composite-Reinforced Mortar Systems,” Journal of Composites Science, vol. 7, no. 8, p. 329, 2023.

[38] A. Kamgar, M. A. Lotfi, and M. H. Kheyroddin, “Estimation of the Ultimate Strength of FRP Strips-to-Masonry Substrates Bond,” Applied Sciences, vol. 13, no. 12, p. 6955, 2023.

[39] F. Saviano, F. Parisi, and G. P. Lignola, “Material aging effects on the in-plane lateral capacity of tuff stone masonry walls: A numerical investigation,” *Materials and Structures*, vol. 55, p. 198, 2022.